

# MSc Programme in Urban Management and Development

Rotterdam, the Netherlands

July 2023

## Houston under Rising Seas: Social and Economic Implications of Climate Change for 2050

Name: Markus Aarup

Supervisor: Qian Ke

Specialisation: Urban Environment, Sustainability & Climate Change

Report number: 1725

UMD 19

## ***Summary***

With climate change rapidly becoming a fixed reality within future predictions, urban centers are facing increasing consequences from threats such as sea level rise and increased extreme weather. The city of Houston, situated on the Gulf of Mexico, is at particular risk. Facing issues such as rapid subsidence, urban sprawl, and population growth as spatio-temporal factors, Houston's precarious situation is compounded by soil composition, exponential population growth, non-centralised land planning, and socioeconomic disparity - in addition to being in an area expecting increasing extreme weather patterns. Given its sizable population of 2.5 million and status as one of the primary economic hubs of the US, understanding the vulnerability of the city and its denizens within the near future is critical for any mitigation strategies to be employed.

As such, the primary goal of this study was to understand the extent, and the threats, socio-economic and physical, that anthropogenic sea level rise poses to Houston, TX. This was tackled through an amalgamation of predictive approaches and GIS to create a digital simulacrum of Houston and its surroundings in 2050. Included in this research are methods such as subsidence topography projection, altitude-based inundation mapping, artificial neural network land use modeling, social vulnerability index impact assessment, and economic damage evaluation. These were carried out across varying Representative Climate Pathway scenarios, their respective sea level rise predictions, and possible storm surge extents.

From this research, the vulnerability of the area was found to be quite high, with worst case scenarios incurring astronomical losses, up to 2,070,655,000m<sup>2</sup> inundated, and 277k people classed as socially vulnerable affected. To counter this and limit future damages, key interventions such as a climate-forward development framework, equitable development regulations, and targeted infrastructure developments have been put forward.

## ***Keywords***

Climate Change, Texas, GIS, Vulnerability, Prediction

### *Acknowledgements*

To begin, I would like to express my utmost gratitude to my supervisor, Qian Ke. Her mastery of flood management and modeling has been an invaluable resource, and her feedback was crucial to my thesis.

I would further like to support my incredible support network, friends and family alike. The following people made my time at IHS truly special. Anarghya Pai Ballambat, Lauren Davini, Radhika Saran, Daoud Banat, Yuval Duer, and Bailey Berdan Gardien have been fantastic friends to me, and I couldn't imagine getting so close to people within just a year. Special acknowledgement goes to Medha Ajay and Patrick Anderson, who in addition to their friendship, have been a huge support through this thesis process.

Finally, I would like to thank my parents and family for their unending support, and the opportunity to accomplish all that I have.

## *Table of Contents*

<b>Summary</b> .....	<b>2</b>
<b>Keywords</b> .....	<b>2</b>
<b>Acknowledgements</b> .....	<b>3</b>
<b>Table of Contents</b> .....	<b>4</b>
<b>List of Figures</b> .....	<b>6</b>
<b>List of Tables</b> .....	<b>8</b>
<b>Abbreviations</b> .....	<b>9</b>
<b>1. Introduction</b> .....	<b>10</b>
1.1 Background Information and Problem Statement.....	10
1.2 Research Question and Objectives.....	13
<b>2. Literature Review</b> .....	<b>15</b>
2.1 Core Concepts.....	15
2.2. Geographic Information Systems (GIS) for Assessing Coastal Inundation.....	16
2.2.1 Inundation Extent Prediction.....	16
2.2.2 Land Use Prediction.....	18
2.2.3 Vulnerability; Analysis and Prediction.....	19
2.3. Economic Impacts of Flooding and prediction.....	21
2.4. Social Impacts of Flooding.....	22
2.6. Potential Outcomes for Planning and Policy.....	24
2.6.1 Utilization of Results for Decision Making and Policy Formulation.....	25
2.7. Conceptual Framework.....	27
<b>3. Methodology</b> .....	<b>30</b>
3.1 Operationalisation Table.....	30
3.2 Research Strategies and Design.....	31
3.3 Study Area.....	32
3.4 Data collection.....	34
3.5 Data analysis method.....	36
3.5.1 GIS analysis.....	36
3.5.1.1 Data processing and Preparation.....	36
3.5.1.2 Inundation Calculation and Validation.....	36
3.5.2 Artificial Neural Network.....	38
3.5.3 Social Vulnerability Index Based Vulnerability Assessment.....	40
3.5.4 Economic Evaluation.....	41
<b>4. Results</b> .....	<b>44</b>
4.1 Inundation results.....	44
4.1.1 Inundation maps under SLR of RCP2.6.....	44
4.1.2 Inundation maps under SLR of RCP 8.5.....	45
4.1.3 Inundation area across RCP's for 2050.....	45
4.1.4 Inundation maps under SLR RCP 2.6, subsidence, and high storm surge.....	46
4.1.5 Inundation maps under SLR RCP 8.5, subsidence, and high storm surge.....	47

4.1.6 Inundation area across RCP's, subsidence, and storm surge for 2050.....	48
4.2. Economic damage.....	49
4.2.1 Projection of Land use change.....	49
4.2.2 Potential Economic Damage (due to climate change and land use change).....	50
4.3 Affected population under Storm Surge Minimum and Maximum Scenarios.....	51
4.4 Interpretation and Discussion.....	52
<b>5. Conclusion.....</b>	<b>56</b>
<b>Bibliography.....</b>	<b>59</b>
<b>Appendix A: Data.....</b>	<b>68</b>
<b>Appendix B: Flood Cost Enumeration.....</b>	<b>70</b>
<b>Appendix C: Results.....</b>	<b>73</b>
<b>Appendix D: IHS copyright form.....</b>	<b>90</b>

## List of Figures

<b>Figure 1:</b> Hazard, Vulnerability, and Risk Interrelationship.....	15
<b>Figure 2:</b> Conceptual Framework.....	28
<b>Figure 3:</b> Study Area, with Counties Delineated.....	32
<b>Figure 4:</b> ANN-CA LULC Transition Model.....	39
<b>Figure 5:</b> Map of Projected Inundation of the Greater Houston Area in 2050, with RCP2.6 Sea Level Rise and Subsidence Predictions.....	44
<b>Figure 6:</b> Map of Projected Inundation of the Greater Houston Area in 2050, with RCP8.5 Sea Level Rise and Subsidence Predictions.....	45
<b>Figure 7:</b> Map of Projected Inundation of the Greater Houston Area in 2050, with RCP2.6 Sea Level Rise, Subsidence, and Storm Surge Predictions.....	46
<b>Figure 8:</b> Map of Projected Inundation of the Greater Houston Area in 2050, with RCP8.5 Sea Level Rise, Subsidence, and Storm Surge Predictions.....	47
<b>Figure 9:</b> Trends in terms of inundation area across Land Use under different scenarios, with subsidence, RCP2.6 and 8.5.....	48
<b>Figure 10:</b> Predicted Land Use Change between 2020 and 2050, by Land Use.....	50
<b>Figure 11:</b> The transition of historical HOLC ratings and current summary SVI ratings.....	54
<b><u>Appendix A</u></b>	
<b>Figure 1:</b> Geographic Information Systems Approach and Methods.....	69
<b><u>Appendix B</u></b>	
<b>Figure 1:</b> Cost (€) per m2 for Commercial Buildings in North America - Structure and Content .....	70
<b>Figure 2:</b> Cost (€) per m2 for Residential Buildings in North America - Structure and Content .....	71
<b>Figure 3:</b> Cost (€) per m2 for Industrial Buildings in North America - Structure and Content..	71
<b>Figure 4:</b> Damage Factor per m2 for Agriculture in North America.....	72
<b><u>Appendix C</u></b>	
<b>Figure 1:</b> Map of Projected Inundation of the Greater Houston Area in 2050, with Projected Subsidence, RCP8.5 Sea Level Rise, and 0.5m & 8m Storm Surge Prediction Applied. Base Density Map of Denizen Population.....	80
<b>Figure 2:</b> Map of Projected Inundation of the Greater Houston Area in 2050, with Projected Subsidence, RCP8.5 Sea Level Rise, and 0.5m & 8m Storm Surge Prediction Applied. Base Density Map of Denizens in Poverty.....	81
<b>Figure 3:</b> Map of Projected Inundation of the Greater Houston Area in 2050, with Projected Subsidence, RCP8.5 Sea Level Rise, and 0.5m & 8m Storm Surge Prediction Applied. Base Density Map of Denizens Unemployed.....	82
<b>Figure 4:</b> Map of Projected Inundation of the Greater Houston Area in 2050, with Projected Subsidence, RCP8.5 Sea Level Rise, and 0.5m & 8m Storm Surge Prediction Applied. Base Density Map of Denizens Burdened by Housing Costs.....	83
<b>Figure 5:</b> Map of Projected Inundation of the Greater Houston Area in 2050, with Projected Subsidence, RCP8.5 Sea Level Rise, and 0.5m & 8m Storm Surge Prediction Applied. Base Density Map of Denizens with No Insurance.....	84
<b>Figure 6:</b> Map of Projected Inundation of the Greater Houston Area in 2050, with Projected	

Subsidence, RCP8.5 Sea Level Rise, and 0.5m & 8m Storm Surge Prediction Applied. Base Density Map of Denizens with Disability.....	85
<b>Figure 7:</b> Map of Projected Inundation of the Greater Houston Area in 2050, with Projected Subsidence, RCP8.5 Sea Level Rise, and 0.5m & 8m Storm Surge Prediction Applied. Base Density Map of Denizens with Minority Status.....	86
<b>Figure 8:</b> Map of Projected Inundation of the Greater Houston Area in 2050, with Projected Subsidence, RCP8.5 Sea Level Rise, and 0.5m & 8m Storm Surge Prediction Applied. Base Density Map of Denizens with African American Status.....	87
<b>Figure 9:</b> Map of Projected Inundation of the Greater Houston Area in 2050, with Projected Subsidence, RCP8.5 Sea Level Rise, and 0.5m & 8m Storm Surge Prediction Applied. Base Density Map of Denizens with Hispanic Status.....	88
<b>Figure 10:</b> MOLUSCE Predicted Output for 2050 Land Use Transition.....	89

## *List of Tables*

<b>Table 1:</b> Operationalisation of Research Concepts, Objectives, and Questions.....	30
<b>Table 2:</b> Socially Vulnerable Peoples within Minimum and Maximum Inundation Storm Surge Extents, with Proportion of Total SVI.....	51
<b><u>Appendix A</u></b>	
<b>Table 1:</b> Data Used - Resolution, Attributes, Sources.....	68
<b><u>Appendix B</u></b>	
<b>Table 1:</b> Costs per Inundated Area, by Depth, on the Basis of Cost-Depth curves.....	70
<b><u>Appendix C</u></b>	
<b>Table 1:</b> Inundation Areas, by Land Use, Across RCP's.....	73
<b>Table 2:</b> Inundation Areas, by Land Use, Across RCP's and Storm Surge Predictions.....	74
<b>Table 3:</b> Inundated Land Uses (m2), per Surge Height.....	76
<b>Table 4:</b> Economic Predictions (in euro) of Maximum and Minimum Storm Surge Scenarios, across Land Uses and RCP's.....	77
<b>Table 5:</b> MOLUSCE-Generated Predicted Land Use Transition for 2050.....	79



## *Abbreviations*

---

IPCC	Intergovernmental Panel on Climate Change
SLR	Sea Level Rise
RCP	Representative Concentration Pathway
GHA	Greater Houston Area
EPA	Environmental Protection Agency
GIS	Geographic Information Systems
DEM	Digital Elevation Model
LULC	Land Use - Land Change
CA	Cellular Automata
ANN	Artificial Neural Network
POC	People of Color
TX	Texas
USGS	United States Geological Survey
LiDAR	Laser imaging, Detection, and Ranging
GPS	Geographic Positioning Systems
MOLUSCE	Modules for Land Use Change Evaluation
ADCIRC-SWAN	ADvanced CIRCulation Simulating Waves Nearshore
NOAA	National Oceanic and Atmospheric Administration
LCMAP	Land Change Monitoring, Assessment, and Projection
SVI	Social Vulnerability Index
ATSDR	Agency for Toxic Substances and Disease Registry'
GRASP	Geospatial Research, Analysis and Services Program
TIN	Triangulated Irregular Network
MOE	Margin of Error
HOLC	Home Owners' Loan Corporation

---

## ***1. Introduction***

Projections by the Intergovernmental Panel on Climate Change (IPCC) indicate the influence of anthropogenic forcing on climate processes post-industrial revolution in progressively increasing global sea levels. The primary mechanisms driving this geological-paradigm-shift include thermal expansion, shifts in natural inland water storage, and the thawing of the world's glaciers and ice sheets (Oppenheimer et al., in IPCC Special Report on the Ocean and Cryosphere, 2019).

While sea level rise (SLR) exact extents are debatable, academia generally concludes that global SLR has reached 21-24 cm since the industrial revolution (Lindsey, 2022). Depending on the greenhouse gas emissions and their associated Representative Concentration Pathway (RCP), the IPCC estimates 43-84 cm SLR by 2100 relative to 1986-2005. The ongoing thaw of Antarctica could contribute up to 28 cm of SLR alone under the worst-case scenario (IPCC, 2019).

Furthermore, whereas SLR singularly may pose risks from a simple inundation standpoint, it is accompanied by a host of comorbidities which exacerbate ecological, social, economical impacts. Coastal ecosystems are prone to destabilization, and the chain-reaction of issues that SLR and its driver, climate change, trigger will have long-lasting repercussions we have barely begun to comprehend (IPCC, 2019). That said, urban developments along the coast are equally, if not more, at risk and are rapidly increasing in factors that compound this vulnerability - such as population booms and urban sprawl (Barros et al., 2005).

### ***1.1 Background Information and Problem Statement***

Houston, one of the United States' key economic hubs, is situated on the coast of the Gulf of Mexico. The sprawling urban mass houses nearly 2.5 million inhabitants and will likely overtake Chicago as the third most populous city in the US by the late 2020's (About Houston, 2023). Houston has a GDP of 463,23 billion U.S. dollars as of 2021, and will continue growing as the primary economic hub of the southern United States (Statista, 2022). Concomitant to its GDP growth, the city of Houston is expected to welcome an additional million people, while the Houston county (Harris) is expected to grow from 4,8 million to 6 million from 2020-2050 (The Texas Demographic Center, 2022).

The development of Houston faces numerous anthropogenic and environmental threats which heighten the city and its citizens' vulnerability to flooding. Among these, rapid subsidence and population growth are at the forefront of spatio-temporal risk factors, compounded by soil composition, exponential population growth, non-centralised land planning, socioeconomic disparity and build quality - all key factors to consider in the the risk profile - in addition to increasing extreme weather occurrence (USGS, 2020; Kim & Newman, 2019; Lieberman-cribbin, Schwartz, & Taioli, 2019; Nielsen-Gammon et al., 2020). This, situated in the context of Texas being the singular most flood affected state of the U.S., indicates an issue of growing concern (Brody et al., 2008).

Subsidence is an increasing issue as groundwater and natural resource extraction continue to support growing human and economic demand, which Houston and its surroundings, given their climate and economic context, suffer heavily from. As temperatures climb, groundwater extraction demand has grown in parallel, leading to the reactivation of fault lines within the Greater Houston Area (GHA), increasing geological activity over time (Buckley et al., 2003). The risks associated with sub-surface extraction are compounded within the GHA, with intra-soil pore spaces at risk of collapse, lacking their previous structural mediums of water, gas, and oil (Galloway, Choplin, & Ingebritsen., 2003).

Houston's clay-based soil aggravates the issue of pore-space collapse, considering its particular characteristic of hydro-fluctuation, with significant rates of expansion and shrinkage depending on ambient water level (Sun et al., 2018). Whereas this poses an issue in and of itself, as groundwater extraction is directly driving clay desiccation and its resultant contraction, the inter-strata layers upon which the GHA sits includes sand, which offers little structural counter to the processes affecting the clay. Soils with a high clay content also offer low permeability, with the resulting low infiltration rates, compounding flood risks (Sun et al., 2018). Furthermore, previously unknown, significant rates (2-4 cm per annum) of subsidence have been reported in certain rapidly developing suburbs in Houston - indicating that the full extent of the issue may be greater than previously understood (Buckley et al., 2003).

While Houston's subsidence issues are primarily driven by the aforementioned anthropogenic, geological interference, a secondary aspect - both affected and the effector in equal measure - is unsustainable urban development. A continuous feedback loop of urban sprawl and

population growth have led to rapid economic growth fostered by natural resource extraction, as well as high rates of urban development across subsidence-prone clay soils (Brody et al., 2008). Although expansivity is not a novel concept to the North American planning mindset, the lack of centralized land planning unique to Houston and the GHA has furthered the issue.

In the absence of a centralized agency for development regulation and coordination, planning and land-use control are relinquished to individual developers and local governance. Without oversight and holistic planning, a fragmented urban landscape has resulted from Houston's high-speed development, in addition to policies aiming to target urban sprawl, sustainable development, and flood risk often facing policy and implementation issues (Bodenreider et al., 2019). A lack of soft-measure control has caused urbanization to spread to areas unfit for construction, such as clay-based floodplains, or existing green areas, wildlife habitats, and farmland, which are all crucial natural services for flood management.

As a product of this ineffectual zoning approach, a host of socioeconomic implications arise. Whereas developers, driven by economic incentives and housing demand, may be keen on developing these at-risk areas, low-income communities, driven from lower-risk areas by gentrification, are often the resulting settlers. Low-income citizens generally have increased risks and vulnerability to flooding due to factors such as limited access to healthcare, resources, and sufficient infrastructure - with substandard building codes allowing for cheap, low-resilience construction (EPA, 2022). Furthermore, the aforementioned inefficient planning system heightens the vulnerability of lower-income communities due to the preferred approach of monetary loss estimation for risk and mitigation implementation, which often overlooks areas with low income due to this simple cost-benefit analysis (Rentschler et al., 2022). Studies have shown that the current flood losses of \$32.1 billion USD in the USA are disproportionately borne by poorer communities, with special regard to those of african-american descent - a stark illustration of the oversights perpetuated by the economic assessment approach (Wing et al., 2022).

Attempting to quantify the projected damages under a worsening climatic system in a critical economic high density urban area, with special regards to that borne by those of lesser economic opportunity, requires a number of projections and simulations. To understand the demographics affected, and the economic extent of this effect, requires projections of future land use, sea levels, and storm surge extents to posit future vulnerabilities and damages to the

evolved urban area. Whereas damages span multiple metrics, the current framework of damage comprehension is primarily focused on indicators easily enumerated and compared. Currently, little public information is offered on projected costs across scenarios, slowing mitigation efforts. On the basis of these findings, policy and infrastructure adjustments could be suggested to minimize the damages to lives and property, safeguarding countless lives within the near future.

While existing research within these topics and areas currently exist, few offer a comprehensive physical, economic, and social analysis on the basis of future conditions to the extent this research aims to do so. Works such as that of Miller & Shirzaei, 2021, Davlasheridze et al., 2019, and Bodenrider et al., 2019, all are focused on varying aspects covered by this research - from Economic Cost-Benefit Analysis Of Storm Infrastructure, Social, Economic, and Geographic Vulnerability Pre- and Post-Hurricane exposure, to Subsidence, Sea-Level Rise, and Storm Surge Scenarios - this research sets itself apart in its inclusion of all three (physical, social, and economic) dimensions, while applying future SLR and storm surge extents to a series of predictions, such as population adjustments and novel land use change.

### ***1.2 Research Question and Objectives***

On the basis of the reasons above, the following research objectives were formulated to guide the research:

1. To establish the inundation extents across sea level predictions within a context inclusive of spatio-temporal elements e.g. urban expansion, subsidence.
  - a. To determine the areas of Houston which are at risk of flooding, across the varying sea level and climate pathway projections
  - b. To estimate and enumerate potential incurred costs associated with the projected inundation extents
  - c. To estimate the demographics influenced across the projected inundation extents

As such, the proposed research question for this thesis is the following:

What is the extent, and the threats - socio-economic and physical - that anthropogenic sea level rise poses to Houston, TX, and its surroundings, given current predictions for 2050, with an understanding of its current risks and vulnerabilities.

With the following sub-questions created to guide the analysis process:

1. How to calculate the urban inundation extent, factoring in the sea level predictions for 2050 - while considering spatio-temporal elements such as urban expansion and subsidence?
  - a. What areas are at risk given inundation across assorted climate pathway scenarios?
2. What are the potential costs associated with the inundation scenarios mentioned above?
3. To what extent are varying vulnerable demographics influenced across inundation scenarios?

## 2. Literature Review

### 2.1 Core Concepts

When conceptualizing the threat of natural disaster on the anthropogenic urban sphere, the concepts of vulnerability, hazard, exposure, and risk are of paramount importance. These concepts are defined as follows; vulnerability, the extent to which a people or development is susceptible to harm, hazard, in reference to the (natural) event with the capacity of causing damage, and exposure, being the presence of peoples, developments, or assets within the area of effect of the event, and finally, risk, the resultant probability interaction across hazard, exposure, and vulnerability (Liu & Chen, 2021). This interrelation of concepts can be found illustrated in Fig. 1 below.

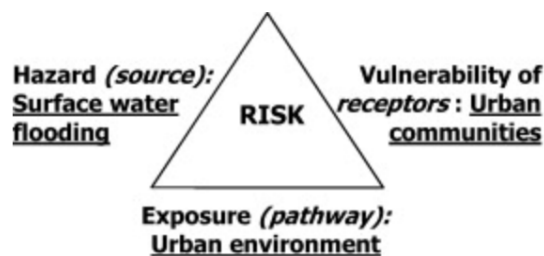


*Figure 1: Hazard, Vulnerability, and Risk Interrelationship.*

*From Kaźmierczak & Cavan (2011)*

With over 300 million people situated in coastal regions, including 20 of the 33 megacities of the world, the low-lying coastal region is one of the areas most susceptible to the multifaceted impacts of climate change and sea level rise (Griggs & Reguero, 2021). For this research, the hazard of interest lies in the flood risk associated with climate change induced SLR and its accompanying intensification of extreme weather events. Per the 2021 IPCC report, by 2050, an expected 0.15 to 0.30m increase in global sea level is to be expected. In conjunction with this rise, sea-level events previously deemed extreme at a once-in-a-hundred-years frequency, will come to pass at an increased magnitude of 20 to 30 times (IPCC, 2021). As such, the frequency and severity of the hazard that the GHA faces is drastically increasing.

Hurricane Ike (2008) and Harvey (2017) both brought mass flooding to the GHA and Galveston bay, which caused significant economic, social, and environmental damages through damaging infrastructure and causing mass acidification of the bay by freshwater introduction (Hicks & Shamberger, 2023). Recent research has revealed that of the high

density blocks in Harris county, 70% of them are located within floodplains that contain a ‘disproportionate’ amount of low-income groups, at increasing risk from SLR and Storm Surges under varying RCP’s (Pulcinella et al., 2019). As such, the GHA is at significant risk, given increasing hazard frequency, with historically proven high vulnerability to flooding, and high number of people with low disaster resiliency within the area of exposure. Therefore, this area and its development are crucial to study in order to best reduce future losses.

## ***2.2. Geographic Information Systems (GIS) for Assessing Coastal Inundation***

Urban flood modeling necessitates the assessment of the risks and implications of the increased risks of SLR. Modeling, a tool unique in its services, can offer advanced insights into urban hydrology by identifying both current and future areas at risk (Cea & Costabile, 2022). Upon these predictions, modeling is further able to assess the viability of various interventions, such as green and gray infrastructure, which shapes both short and long term planning - granting emergency services increased responsivity, policy makers increased decision making power, improved infrastructure resilience, and more (Wu et al., 2020). Flood management, specifically flood disaster management, traditionally includes the following stages; prediction, preparation, prevention, and damage assessment and mitigation - with GIS flood modeling having proven efficient and irreplaceable across each stage (Opolot, 2013). Given the predictive nature of the research, the vast geographical area of interest, and the depth of information being processed, a geographic information systems (GIS) approach was best suited for this research.

This research applied GIS to the prediction of the following; inundation extent, land use development, vulnerability assessment, and economic loss. The following paragraphs will outline the current state-of-the-art techniques used, their key differences, and limitations.

### ***2.2.1 Inundation Extent Prediction***

Inundation prediction utilizes a number of physical (hydrodynamic) and GIS models across research, given different use cases and requirements for data. These inputs often include river discharge rates, surface roughness, land use, soil type, Digital Elevation Models (DEM), drainage basin demarcations, and rainfall patterns. Frequently, the majority of this data is sourced through remote sensing, a tool often found synonymous with the majority of recent GIS work (Opolot, 2013). Furthermore, these inundation models frequently include



storm-runoff modeling, increasing their complexity (Chen et al., 2009). Current models in use include; WetSpa, HYDROTEL, LISFLOOD, TOPMODEL and SWAT. Some recent models have emerged utilizing artificial neural networks, a method discussed in the land use prediction section below (Opolot, 2013, Kia et al., 2012). These methods generate probabilistic inundation outcomes with an incredibly high degree of accuracy and depth of understanding, which is of great importance when creating long-term plans and policy. Given the large degree of data and processing the models are granted, the application of such models often yield concrete policy and strategy reform. Examples of this include modification of basin-scale irrigation control policies in northern Germany, optimisation of urban drainage systems for climate change on Haidian Island, China, and wetland management strategies in Quebec, Canada (Maier & Dietrich, 2016; Xu et al., 2020; Tiné et al., 2019)

While these models can offer unparalleled and invaluable insights, they nevertheless suffer numerous drawbacks, namely their data and processing requirements. Physical models often demand high resolution data, frequently inaccessible, on physical aspects such as infiltration conditions, topography, and sewer conveyance. The latter alone requires detailed information on pipe specifications, locations, boundaries and more, often posing a significant challenge to the implementation of such high quality models within urban environments. Furthermore, the simulation of hydrological activity within such complex environments requires significant computation costs, demanding long wait times and advanced hardware, making simulations often unsuitable for emergency situations (Zhang & Pan, 2014). In addition, current and previous urban modeling further share a common weakness in their reliance upon historical weather patterns for forecasting - a practice increasingly inaccurate given the destabilization of atmospheric processes (Wing et al., 2022).

Simplified GIS methods and models still hold significant value and provide similar insights - at much decreased cost. One of such methods involves altitude-based inundation calculations. As seen in Zhang & Pan (2014), non-source flood allocation requires all points below the given flood elevation be given the water level of the flooded area. Although physical models are often utilized for flood forecasting, they require extensive information and data, and errors and uncertainties may compound throughout the modeling process. GIS models, however, significantly decrease input and processing demands (Ji et al., 2012, Seenath et al.,

2016). A GIS approach was similar to that of Zhang & Pan (2014) utilized for the purpose of this study, given data accessibility, processing, time, and scope considerations.

### ***2.2.2 Land Use Prediction***

In order to assess the impacts of predicted inundations, with global urban area projected increasing by 66% in 2050, predictive land use land change (LULC) models become a necessity for future analysis (United Nations, 2014). LULC models function on the basis of past, present, and future projection determinants, and provide valuable insights into development trajectories and outputs. Previously, LULC models have provided valuable insights into large-scale transitions in fields including conservation work, studying aspects such as the degradation of the Meighan Wetland or Chunati Wildlife Sanctuary or natural resource allocation and planning, as the case of Sumatra (Ansari & Golabi, 2019; Islam & Jashimuddin, 2018; Saputra & Lee, 2019).

Spatial distribution models such as Dinamica, CA-MARKOV, SLEUTH cellular automata, CLUE-S, and more have been used by researchers for LULC projections and analysis (Muhammed et al., 2022; Kamaraj & Rangarajan, 2022). Each model has unique strengths and best-use applications; however, cellular automata (CA) models are the most prevalent given their ability to reflect non-linear probabilistic LULC information within the spatial domain, when paired with an artificial neural network (ANN) model (Kamaraj & Rangarajan, 2022). With cellular automata as the methodological driver, CA-ANN models predict spatial shifts through per-pixel relativity analysis, considering its own and neighbors behavior across time. Such a CA-ANN model is employed by the tool MOLUSCE, making one of the most prevalent choices in temporal LULC shift projection - used across a number of scenarios such as deforestation, crop conversion and expansion, and more (Kamaraj & Rangarajan, 2022).

Despite their usability profile, these models are embedded with a number of limitations that are predominantly linked to the nature of their source data. The input data faces numerous challenges in its creation and processing, such as satellite pre-processing or the shifting of land use classification extents and definitions, which affects the validity of the resultant model. Additionally, the calibration of the independent and dependent variables within each predictive model remains a challenge within the LULC prediction process, along with issues within the validation step (MohanRajan et al., 2020).

Given the high degree of existing urbanization and lack of centralized regulatory processes for planning, the land development of the GHA raises concerns about sustainable land development - particularly given its large population of vulnerable people, and subsidence and flood risk. In order to best understand development patterns and future development, LULC modeling is crucial to the understanding of predicted impacts in this research.

### ***2.2.3 Vulnerability; Analysis and Prediction***

The concept of flood vulnerability is influenced by the same factors which affect a person, namely; environmental, economic, social, and political. Additional factors, such as infrastructure, policy, settlement conditions, economic patterns, and social inequalities are core determinants of the extent to which a group is vulnerable to floods (Nasiri et al., 2016). This interrelationship can be understood through the three base constituents of vulnerability - susceptibility, exposure, and resilience. Susceptibility is a measure of the probability of a people, environment, or infrastructure to be compromised as a function of its fragility. Exposure, much the same as the definition used in the risk triangle in 2.1, is the people or developments within the area of the natural disaster. Resilience, ultimately, is in reference to the system's ability to weather shocks, as a measure of coping and adaptive ability (Beevers et a., 2016). The joint analysis of these three elements allows for the assessment of an area or peoples vulnerability, allowing for the guidance of governance and emergency response services.

Historically, flood vulnerability analysis has progressed through a number of trends and methodologies, integrating advances in geospatial technology and techniques as they emerge. Past flood vulnerability assessment was oriented towards site characteristics, inundation depth, and topography. Due to the lack of methodological standardization for site specific assessments, these approaches were shifted within the geospatial technology revolution - applying GIS, remote sensing, 3-D hydrological models, and artificial intelligence techniques (Nasiri et al., 2016).

Within situations of lacking or inadequate flood data, non-parametric approaches are employed. The majority of vulnerability assessment employs indices, models, and frameworks, such as the coastal vulnerability index, sustainable livelihood analysis, multi criteria analysis, and logical tree models (Balica et al., 2009). Generally, the approaches used

can be classified as one of the following four methods: curve-based, disaster loss data, computer modeling, and indicator-based.

The curve method is reliant upon fragility or damage curves to assess and study the relationships between flood risk and the elements of interest, often focusing on case studies with high degrees of documentation. This data enables the creation of step-damage curves for potential damages within the area (Romali et al., 2015). Unfortunately, given its reliance on previous knowledge and data, its applicability is often limited to specific areas, in addition to limiting its reliability and applicability in novel applications (Nasiri et al., 2016).

The disaster loss data method applies to future scenarios on the basis of direct application of data from previous, real, flood events. Albeit simple and effective, it suffers from limitations of its source data, such as unevenly recorded data or processing errors carried forwards (Nasiri et al., 2016).

Computer modeling, or GIS, can offer a high-resolution insight into the vulnerability of an area, both in real time and predicted. Utilizing the hydrological modeling methods mentioned previously, this approach grants a particular advantage in understanding impact extent, and offers significant customisation on a case-by-case basis (Rehman et al., 2019; Chan et al., 2022). However, as previously mentioned, these models similarly suffer from the data requirements that offer them their strength in details. Furthermore, given the number of assumptions required within computer modeling approaches, the linkage between predicted maps and actual flood damage levels may suffer (Nasiri et al., 2016).

Finally, indicator-based methods provide an assessment of vulnerability through the use of flood reflexive data. This commonly used approach is often used by policymakers due to its ability to prioritize measures and provide a basis for rapid risk response planning (Messner & Meyer, 2006). This approach is reliant upon complex indices that, with and without, weighting allows for inbuilt bias. Furthermore, the creation of these indices causes indicator-based vulnerability assessment to struggle with issues such as aggregation methods, uncertainty, standardization, and more.

Across studies of the GHA, most research has employed the latter two methods, with some interrelation of approaches also occasionally found (Bodenreider et al., 2019). Some studies

have utilized benefit-transfer methods on the basis of the disaster loss method, wherein previously completed research is applied to the novel solution (Quagliolo et al., 2023). Nevertheless, validity is occasionally called into question and their utilization suffers (Davlasheridze et al., 2019).

### ***2.3. Economic Impacts of Flooding and prediction***

Within flood assessment, the shift from flood hazard to flood risk management has been a significant development that places emphasis on flood damages taking place within a period of time with a certain probability, over the direct control or management of the flood hazard itself. Flood damages fall into four groups; direct (stemming from the physical flood contact of humans or property), indirect (damages caused outside of the flood event, from direct impacts), tangible (assessable within monetary terms), and intangible (outside of monetary assessment). These assessments are carried out across varying spatial scales from micro- (individual buildings) to macro-scale (municipalities, regions, countries) (Messner & Meyer., 2006).

Economic assessment of flood damages are carried out by numerous parties, with applications ranging from disaster relief to insurance compensation (Merz et al., 2010). Additionally, these evaluations are a crucial component of the cost-benefit analyses, since weighing the advantages of mitigation against its costs is key in policy-making decisions (Kok & Costa., 2021). The most commonly used procedure for direct monetary flood damage assessment involves classifying elements at risk, analyzing exposure and asset value, and evaluating susceptibility to flood impact. Both relative damage approaches (damage share) and absolute damage approaches (monetary amount per risk element) are used (Merz et al., 2010). These complexities and considerations are accounted for in economic assessments are imperative for flood risk management and decision making to be effective.

Contemporary economic flood and subsidence assessments generally lack standardized frameworks, leading to variability in study characteristics, geographical origin, and economic assessment approaches (Kok & Costa., 2021). While significant progress has been made within damage data collection and model development, a misalignment of the applicability of damage assessments and the quality of current models and datasets persists. Damage assessments depend on various assumptions and involve economic evaluation challenges, such as choosing between replacement costs or depreciated values. Model validation,

uncertainty analyses, and scrutiny of inputs and assumptions are essential for robust damage modeling (Merz et al., 2010; Kok & Costa., 2021).

As such, while advanced models may be able to offer unparalleled insights, they similarly suffer from their inputs and parameters. Due to this, the utilization of flood damage curves - functions of cost per land use per inundation depth, created on the basis of historical events and expert judgment - are commonly used as an alternative. Given the prevalence of the approach and research devoted to its creation, this approach will further be employed for this study - in lieu of novel assessment.

Noteworthy is the apparent lack of peer-reviewed economic assessments in research of the GHA. With no quantified value of damages easily found, papers opt to somewhat extrapolate on damage figures from past events, instead of generating unique predictions. As such, there is currently little information on exact potential costs.

#### ***2.4. Social Impacts of Flooding***

Flooding caused by sea level rise has significant social consequences - particularly in coastal areas and megacities. With a large portion of global urban populations residing in low-lying areas, the most vulnerable are those in poverty, or people of color (POC) residing in slums or informal settlements. To exemplify this, 35% of the urban population in Manila, the Philippines, consists of informal settlements at coastal flood risk (Vojinovic & Abbott, 2012). SLR flooding can have numerous impacts on human wellbeing, including public health, displacement pressures, social equity, and community resilience, putting those with the least resources at the most risk.

The increased density of urban living, compared to rural, can contribute to the generation of risk and vulnerability to natural disasters. Higher population densities increase the concentration of energy and transportation routes in residential areas, which makes them more vulnerable. Moreover, living in crowded conditions can hinder relief efforts during floods due to traffic congestion (Pulcinella et al., 2019). Cities, as complex systems, can exhibit unpredictable behavior during and after disasters, with certain groups within urban populations potentially becoming targets for exploitation and repression. Thus, the scale of a community is a particularly key determinant of flood capacity - with mega cities (> 10 million) often experiencing the greatest losses, often attributed to high population densities

and informal settlements (Vojinovic & Abbott, 2012). Additionally, megacities often attract large-scale industrial settlements, which can compound both the magnitude and frequency of hazards. Therefore, rapid population growth and poverty prevalence can determine and impair a city's crisis adaptation capacity.

The high rates of informal settlements and urban poverty are often directly linked to historical factors, frequently stemming from the exclusion of low- and middle-income residents from the formal housing market, through economic inaccessibility and inappropriate financial legislation. Ultimately, these pressures force the settlement of hazardous or locally unwanted land uses, placing an unequal burden from environmental hazards on POC, marginalized, and disenfranchised groups (Bodenreider et al., 2019; Chakraborty et al., 2019; Collins et al., 2018). A UK based study revealed that 81% of flood vulnerability could be attributed to being in poverty, a minority, having dependents, or old age (Każmierczak & Cavan, 2011).

Poverty, a critical aspect of flood risk, in part determines the degree of loss incurred by different population segments through preparedness - defined as all actions taken in the attempt to reduce the potential impacts of disasters. Whereas wealthier individuals can afford better housing conditions in safer locations and maintain comprehensive insurance coverage (resulting in lower losses compared to the poorer population), economically disadvantaged residents lack similar financial securities (Collins et al., 2019). Socioeconomic factors including race, class, ethnicity, and gender, further contribute to the formation and magnitude of disaster risk through their influence on employment and socioeconomics (Pulcinella et al., 2019; Vojinovic & Abbott, 2012).

Socially vulnerable households often exhibit lower degrees of hurricane and earthquake preparedness. In the USA, POC and poverty-struck homeowners are less likely to own earthquake or flood insurance and are restricted in disaster resources, knowledge, and skills, leading to decreased evacuation order compliance (Pulcinella et al., 2019; Collins et al., 2019). Ultimately, these factors compound, leading to increased rates of property damage, injury, and death among socially vulnerable peoples.

Traditional flood risk assessments have primarily focused on physical vulnerability and damages, while neglecting the vulnerability of inhabitants and their capacity to adapt and respond to hazards. Social vulnerability plays a crucial role in determining the feasibility of

flood risk management policies. Comprehensive assessments that consider both hazard impacts and social vulnerability provide valuable information for evaluating risk mitigation policies, evacuation plans, and insurance coverage. Linking social vulnerability to risk management strategies can improve the effectiveness of flood risk reduction measures (Vojinovic & Abbott, 2012). Given the approximation the above factors offer regarding social vulnerability and preparedness, they have been selected for application of flood impact within this research.

Within the GHA, the above trends are applicable with the exception of the prevalence of informal housing. A study focused on Harris County, TX, revealed that 70% of densely populated census block groups are located within the floodplains, including a disproportionate amount of low-income and minority groups (Pulcinella et al., 2019). Some research disputably does not find any particular racial and ethnic disparity within those affected by flooding in Houston, but there is near unanimous agreement that factors such as age groups, education level, and income level are factors of influence (Mazumder et al., 2022; Collins et al., 2019)

Taken together, these findings emphasize the urgent need for comprehensive and equitable flood risk management strategies. Targeting support for vulnerable communities, and integrating mitigation efforts that consider the specific challenges faced by socially disadvantaged groups, are crucial steps towards reducing social vulnerability and promoting resilience in the face of flooding events. Addressing these issues will contribute to more equitable outcomes that ensure all residents equal access to protection, resources, and opportunities to mitigate the impacts of flooding.

## ***2.6. Potential Outcomes for Planning and Policy***

This section focuses on potential practical and policy applications of the research, with an emphasis on economic damage enumeration and social vulnerability assessment within decision making and policy formulation. Specifically, this section aims to emphasize how these research insights on reducing damages for at-risk groups can contribute to effective urban planning and policy reform.

Given the multifaceted nature of climate-change SLR, the role of economic evaluation and social vulnerability assessment cannot be ignored. Together these components provide crucial



insights into the potential impacts of flood events on both physical infrastructure and vulnerable communities. While damage enumeration offers a strong quantitative understanding of the economic ramifications of flooding, - social vulnerability assessments underlines the populations at the greatest risk and ensure the efforts are best executed. As such, this research could aid in ensuring equity and inclusion within disaster management - aspects often overlooked.

### ***2.6.1 Utilization of Results for Decision Making and Policy Formulation***

The applied methodologies and concepts, and their resultant findings, offer a myriad of practical applications that are critical for guiding decision making and policy formulation across numerous levels. Flood management can be considered through structural and nonstructural approaches, and pre- or post-flood. Structural approaches are often infrastructure responses, involving the basic hydrological principles of storing, diverting, or confining floods. Non-structural approaches consist of soft measures such as education, forecasting, planning, and building codes. Pre-flood activities are key to disaster mitigation, in which vulnerable areas are identified, preventative infrastructure is built, and awareness is spread regarding preparedness. Finally, post-flood activities include reconstruction, recovery, first aid, and flood management measure review (Nasiri et al., 2016). With these principles in mind, the following set of findings were devised, in tandem with existing strategies and research being done;

1. **Creation of a Future Planning Framework:** The insights gleaned from the GIS inundation predictions, paired with LULC modeling and damage costs, could be put towards the development of comprehensive urban planning and infrastructure design frameworks. Through the integration of flood risk assessments into urban processes, decision makers can make informed decisions on prioritization of resilient land use, discourage the development of high-risk areas, and promote sustainable development practices. A similar outcome was successful in Aveiro, Portugal. Here, cost-benefit calculations and software (including GIS) was used to create a new spatial biophysical-economic framework, allowing for the inherent assessment of nature based solutions in urban flood risk mitigation under climate change (Quagliolo et al., 2023).
2. **Policy Alteration for Equitable Urban Development:** The identification of vulnerable communities offers an opportunity for city and zoning policy to be reviewed,

promoting more equality within urban development. Through dedicating efforts towards equitable resource access, affordable housing outside of hazardous areas, and improved social services, policy makers can take on reducing the disparities that magnify the effects of disaster on disadvantaged populations.

3. Policy Alteration for Poverty Alleviation: Serving as a basis for poverty targeted policy reforms, the economic damage evaluation stands to be a useful tool. Through the quantification of economic losses suffered by the vulnerable communities, this information could serve as a starting point for policy makers to shift fund allocations for targeted infrastructure developments, job creation, and the development of social safety nets, nurturing resilience and preparedness of those in need.
4. Increased Inclusivity in Disaster Planning: Through the integration of the social vulnerability assessment into existing emergency response planning, the preparedness of socially vulnerable groups can be enhanced. Made possible through the tailoring of evacuation plans, communication strategies, and support systems to the needs of the affected marginalized groups, policy makers can maximize responsiveness, and minimize damages and loss of life under flood scenarios.
5. Cost-Benefit Analysis for Decision Makers: Using the economic damage evaluation results to create a cost-benefit equation, decision makers are empowered to make better decisions in evaluating various flood risk mitigation strategies' feasibility and impacts. Through the comparison of cost of implementation and potential benefits, decision and policy makers could allocate increased resources towards measures such as; green infrastructure, flood barriers, and early warning systems. Additionally, the enumeration of potential costs could dissuade continued extraction of ground resources, with subsidence being a contributing factor to the risk of the GHA.
6. Guided Physical Infrastructure Responses: working in tandem with the cost-benefit equation, the GIS inundation insights could be applied in the design and implementation of physical flood mitigation infrastructure. By highlighting areas of particular risk across different flood scenarios, these findings can be used to inform the planning of sea walls, sea spines, and other climate-proof protective measures against SLR and storm surges. A similar approach has been employed by Davlasheridze et al., (2019), focusing on Sea Spine implementation alone.

In conclusion, the research, methods, and outcomes explored can have numerous implications for decision making and policy formulation in the face of climate change-induced sea level

rise. The application of economic damage evaluation and social vulnerability assessment can guide the creation of frameworks, policies, and strategies that prioritize equitable development, enhance resilience, and mitigate impacts of flooding on both physical infrastructure and vulnerable communities. By integrating these insights into urban planning and disaster management efforts, policy makers can pave the way for a more sustainable and resilient future.

## ***2.7. Conceptual Framework***

In summary, this literature review provides crucial insights into the complex challenges and social implications that sea-level rise-induced flooding poses for the GHA and beyond. Spanning a range of topics, from core concepts such as those of risk, hazard, vulnerability, and exposure, the application of various methods - such as GIS - for the assessment of coastal inundation, to the social and economic impacts of flooding, this review serves as a conceptual foundation for this research. Through analysis of these topics, several conclusions can be drawn in addition to topics identified as areas for further investigation.

The key findings of the literature review are as follows:

1. **Risk Dynamics:** The interplay between vulnerability, hazard, exposure, and risk has been elucidated, calling attention to the necessity for a comprehensive understanding of these concepts in evaluating the threats posed by SLR. The GHA's susceptibility to flooding and storm surges, coupled with a rapidly growing population and precarious urban development trajectory, accentuates its vulnerability to climate-related hazards.
2. **Computerized Projections as a Tool:** GIS has emerged as an indispensable tool for predicting coastal inundation, land use change, and assessing flood risk within modern research. Its application enables advanced insights into urban hydrology, aiding in the identification of high-risk areas and informing decision-making processes. Hydrodynamic process models offer further insights, but at the cost of time, resources, and input demands. Land use transition modeling can bring a temporal aspect to these outputs, increasing their odds of accurate prediction.
3. **Economic Implications:** Economic assessments of flood damages highlight the substantial costs associated with flooding, revealing the need for robust mitigation strategies and cost-effective solutions. However, a universal standardized framework for economic assessment is lacking, leading to variability in study characteristics and approaches.

4. **Social Vulnerability:** Socioeconomic factors, including poverty, race, and inequality, play a crucial role in determining vulnerability and disaster preparedness. Social vulnerability assessments are essential for promoting equitable disaster management strategies. Vulnerable people are generally disproportionately affected by natural disasters through inequitable urban development.
5. **Planning and Policy Implications:** The findings from this literature review have direct implications for urban planning and policy formulation. They suggest the importance of integrating economic damage enumeration and social vulnerability assessment into decision-making processes. These insights can guide the development of comprehensive urban planning frameworks, equitable policy reforms, poverty alleviation measures, and targeted disaster response strategies.

These findings have become the basis for the conceptual framework of this research, in part adapted from the framework utilized in the study by Liu & Chen (2021) (Fig. 2).

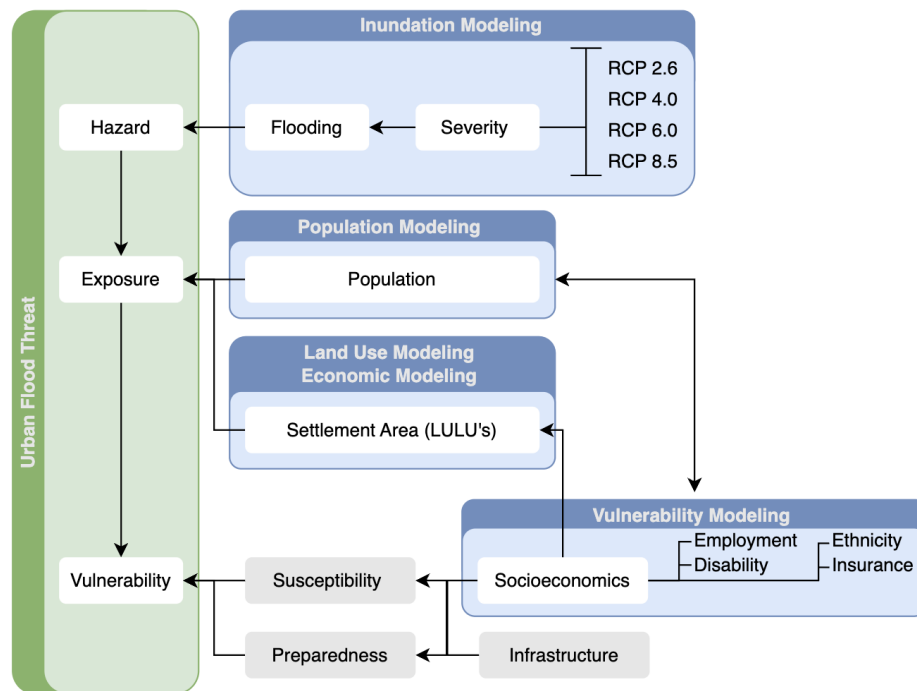


Figure 2: Conceptual Framework. Source: Internal, Author Made

While this literature review provides a robust foundation for understanding the challenges posed by sea level rise-induced flooding, several research gaps and areas for further investigation have been identified:

1. **Integrated Frameworks:** Future research could focus on developing integrated frameworks that combine economic damage assessment, social vulnerability analysis, and GIS-based predictions to provide a holistic understanding of flood risk and inform policy formulation.
2. **Universal Economic Assessment:** a global standardized assessment framework for flood damages could bolster the accuracy and inter-study comparability of future research. In improving cost-benefit comparison extents, decision-making and resource allocation could be done more efficiently by drawing on directly comparable similar studies.
3. **Long-Term Economic Impacts:** As the influences of SLR and climate change will only grow, dedicated exploration of long-term economic consequences of its resultant flooding on local economies would be crucial for future safeguarding efforts. Analysis of impacts on property values, job markets, and business practices could all provide valuable insights for potential policies.
4. **Community Resilience:** While existing research stands within this field, further analysis of confounding factors in community resilience could prove critical to ensure all communities are equally safeguarded. Given the innate degree of variability between communities, cross comparison and extrapolation of research may face barriers, and as such the understanding of factors including access to resources, social networks, and education, would provide a strong foundation for future novel research and targeted interventions - enhancing disaster preparedness.
5. **Equitable Disaster Response Planning:** Targeted research focused on equitable disaster response and recovery for socially vulnerable peoples could perhaps yield knowledge key to the conceivment of disproportionate impact mitigation plans.

In essence, this literature review serves as a critical stepping stone in the broader pursuit of effective flood risk management and resilience building in the face of sea level rise. By leveraging the insights gained from this review, policymakers, urban planners, and researchers can collaborate to develop targeted strategies that enhance the GHA's capacity to mitigate, adapt to, and recover from the multifaceted challenges posed by sea level rise-induced flooding.

### 3. Methodology

This study utilized a number modeling and analysis techniques to generate SLR and storm surge inundation scenarios, across RCPs. This is done with the highest accuracy possible with regard to predicted land use development, subsidence, and population vectors. Full processes are available in Appendix A, Figure 1.

#### 3.1 Operationalisation Table

The variables for this research have been identified using existing literature and research on the field of flood risk, prediction, vulnerability, and economic evaluation. The indicators used in the process of answering the research questions and objectives set above are provided in the table below.

Table 1: Operationalisation of Research Concepts, Objectives, and Questions

Research Objective	Research Question	Dependent Variable	Independent Variables	Indicators	Data Collection Method	Data Analysis Method
To establish the inundation extents across sea level predictions within a context inclusive of spatio-temporal elements e.g. urban expansion, subsidence.	How to calculate the urban inundation extent, factoring in the sea level predictions for 2050 - while considering spatio-temporal elements such as urban expansion and subsidence.	Inundation	Topography, Subsidence, Sea Level Rise, Storm Surge, Land Use	Inundation Extent, Inundation Depth	Topography, Subsidence, Sea Level Rise, Storm Surge height, Land Use	GIS analysis ANN machine learning approach
To estimate and enumerate potential incurred costs associated with the projected	What are the potential costs associated with the inundation scenarios mentioned above.	Economic Consequence of Flooding	Inundation Depth, Land Use, Flood Depth-Cost vulnerability	Cost of Inundated Area per Land Use	Land Use type and maximum economic damage/cost, Flood Depth-Cost	GIS analysis and Depth-Cost Function Analysis

---

inundation					Data	
extents						

---

To estimate the demographics influenced across the projected inundation extents	To what extent are varying vulnerable demographics influenced across inundation scenarios.	Social Consequence of Flooding	Inundation Extent, Demographic Distribution	Number Of Socially Vulnerable People Affected By Flood Extents	Social Vulnerability Indices	Spatial analysis of Vulnerable Peoples distribution within Inundation Extents
---	--	--------------------------------	---	--	------------------------------	---

---

### ***3.2 Research Strategies and Design***

Based on the literature above, the Geographic Informations Systems approach was deemed the most fitting choice to answer the research questions posed. This exploratory research aims to assess extents, and as such lacks a dedicated hypothesis. Said hypothesis can be created post-analysis in future research, once extents and mechanisms have been properly modeled and assessed.

This research creates a predicted set of storm scenarios for the GHA within 2050, utilizing varying GIS components, existing data, and simulations to construct this facsimile. For inundation extents, future subsidence was predicted - based on existing rates - with established RCP SLR extents applied, and ultimately validated against established SLR extent predictions. Future land use was predicted through a model, which was validated against a snapshot excluded from the training data. Economic modeling was carried out on the basis of the intersection of depth and land use. Finally, social vulnerability modeling was carried out through overlay of demographic distribution data and inundation extents.

Within this research, there are a number of limitations that are to be expected - predominantly methodology based. To start, with GIS, the outputs can only ever be as accurate as the input data. While public source data is of sufficiently high quality, given the hydrological nature of this research, the accuracy of inundation is significantly determined by inputs. Furthermore, the modeling approach to be employed, as with any model, is a drastically simplified reflection of reality, and as such will lack certain accuracy or dimensions. Lastly, as with any methodology which utilizes its own iterative outputs for the next step, there is a risk of inaccuracies compounding. To counter this, the methodology was devised on the premise of

simple, but effective, approaches - with the highest publicly available resolution data employed.

### 3.3 Study Area

Whereas Houston may be the primary economic and demographic center for Texas along the coast, given the nature of inundation and sea level predictions, the area of interest for this study were the Harris, Chambers, and Galveston counties. This was done in order to encapsulate the entirety of the Galveston Bay, its surrounding lands, and the majority of Houston (Figure 3)

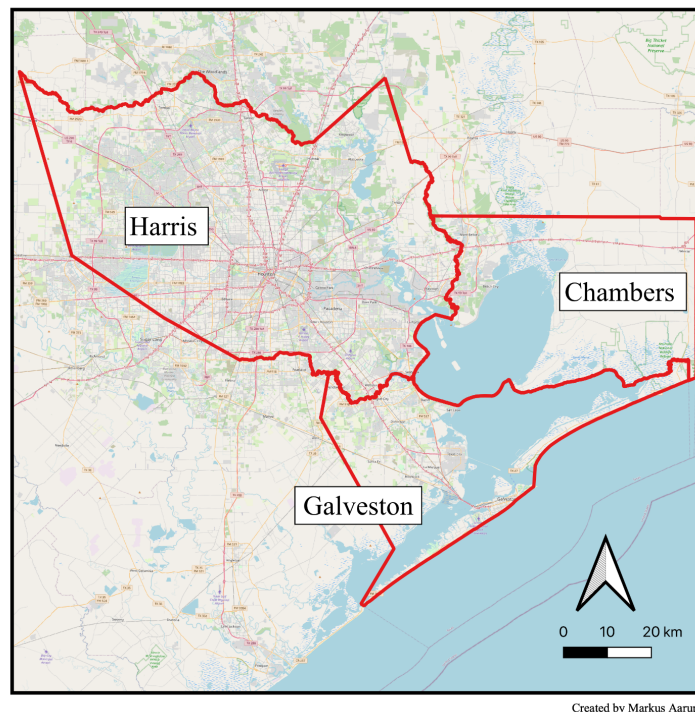


*Figure 3: Study Area, with Counties Delineated*

These three counties represent a collective of 85.8 km<sup>2</sup>, and contain approximately 5.3 million denizens as per 2022 (You & Potter, 2022). Since the 1900's, within a 100km radius of the center of Galveston Bay, this area has experienced 21 tropical cyclones, with 8 of these being category 3 or greater (Bass et al., 2018). Particularly since the 2008 Hurricane Ike, both local and regional surge mitigation strategies have been discussed to minimize future loss of life and land. While existing infrastructure exists, its protection is limited to select areas. This risk is further compounded through the sedimental compaction of the area, with the northern



and western extents of Houston having undergone up to 27 cm of subsidence from 2018-2022 (Ramage, and Adams, 2022).

Within the tri-county area, the major land uses, as per USGS land use classification, is urban (40.4%), with cropland (20%) and wetland (13.9%) being the subsequent highest (Pengra et al, 2021). These counties, Harris and Chambers in particular, feature a vast variability within their ecologies and notable land features, such as numerous major bayous such as Buffalo, Brays, and White Oak, in addition to multiple large parks, nature reserves, and wildlife refuges (Henson, 2020; Kleiner, 2020). Important to note is prevalence of marsh and semi-aquatic features, with regard to flood capacity. Galveston boasts a multitude of parks and reserves as well, being composed of several barrier islands along the Gulf Coast - with these islands being bisected by critical waterways such as Galveston Bay and the Houston Ship Channel (Kleiner, 2021).

The Houston Ship Channel is one of the busiest ports within the United States, providing a major economic artery for the area through the provisioning of trade of goods, and more importantly, natural resources. With the exception of Galveston, whose income is primarily dependent on tourism, the core economic drivers of Harris and Chambers lie in natural resources and mining, trade and transportation, and utilities (Comptroller Texas, 2022). However, despite the \$24.7 billion that the petrochemical industry generated in Texas in 2022 - with the majority of it coming through Houston, an average of 20% of households lie below the poverty line (Drane, 2023). Particular note should be paid to the hispanic populations who, of the 1.5 million which contribute to Harris' total 4.8 million inhabitants, a staggering 412,000 (28%) fall below the poverty line (United States Census Bureau, 2021). This trend can be seen echoed in Chambers, with 44.27% of those in poverty being Hispanic, while in Galveston the demographics are shared between those of African American descent along with those of Hispanic - at around 20% each. With reference to the socioeconomic implications outlined previously, placing those with lesser economic capacity at greater risk, the imputation of the disproportionate risk that the Hispanic and African American communities are at is one which is examined through the following geographic information systems analysis.

### ***3.4 Data collection***

For this research, a number of different data sources were required to create an in-depth analysis of exposure and vulnerability of the GHA. Each source is included in Appendix A:Table 1, and described below.

The basis of the flood extent calculations were the following three sets of data; the DEM, for altitude calculations, the subsidence data, to model the future DEM, and the storm surge predictions.

The Digital Elevation Model (DEM) chosen was dependent on its characteristics, specifically its resolution and its degree of currency - both of which are core to the accuracy of this research, given that the DEM becomes the basis for all inundation projection. As such, the highest resolution contour mapping technology was selected - LiDAR (laser imaging, detection, and ranging). Utilizing the temporal differential between laser output, and its subsequent refraction, LiDAR represents the leading DEM technology, and the USGS was able to provide a contour file at a 1/3rd of an arc-second, or 10x10m, resolution from 2021 (USGS, 2021).

Subsurface sediment cumulative compaction data, also per the USGS, was sourced by analog means through a network of extensometers across the Chicot and Evangeline aquifers - the primary subsurface features spanning the GHA. The resultant relativity outputs are generated 12 times per annum through numerous monitoring stations, adding to a dataset spanning from 1973 onwards. However, since 2017, this data has been supplemented through GPS based monitoring - enriching the subsidence point base mesh (Ramage and Adams, 2022).

Storm surge predictions, on the other hand, were extracted from novel research from Bass et al., (2018) simulating potential tropical cyclone intensities and sizes. For a total of 80 different simulations of 20 storms at four different landfall locations surrounding Galveston Bay, a ADvanced CIRCulation (ADCIRC) and simulating WAVes Nearshore (SWAN) (ADCIRC-SWAN) numerical model was employed. While this study focused on both 2050 and 2100 and created hypothetical ranges spanning all the way up to 12 meters for 2100, simplified 2050 storm surge values were used from a resultant study - Miller & Shirzaei, 2021. These were used in tandem with the RCP sea level rise predictions for the inundation

mapping. For validation purposes, the SLR extents from the Digital Coast files from the NOAA's Office of Coastal Management was used for the GHA area (NOAA, 2022).

For future land use modeling, the MOLUSCE plugin was used. The procedure of ANN-CA land use change prediction begins with data input, wherein high-quality training data must be fed to the model to ensure optimum results. In this study, land use data was found which sat at the intersection of resolution and timescale - with clearer models available, at the cost of time scale encapsulated. As such, the USGS Land Change Monitoring, Assessment, and Projection (LCMAP) data was selected - offering both a workable resolution of 30x30m from the Landsat projects, and a decent time range, spanning from 1985-2018 (Pengra et al., 2022).

In order to assess the social domain influenced by the projected inundations, data from the Agency for Toxic Substances and Disease Registry's (ATSDR) Geospatial Research, Analysis and Services Program (GRASP) was employed to offer crucial insights (CDC, 2020). Created in 2011, GRASP was created to bolster public health efforts within hazardous event occurrences, ensuring quick and precise responses to those most vulnerable.

Based upon the U.S. Census data, GRASP offers uniquely high resolution data across 16 key social factors, such as poverty, vehicle access, and more. For the purpose of this study, on the basis of the literature previously discussed, the following social indices were selected for inundation analysis; population, persons below 150% poverty estimate, unemployment rate, housing cost-burdened occupied housing units with annual income less than \$75,000 (30%+ of income spent on housing costs), uninsured in the total civilian noninstitutionalized population estimate, civilian noninstitutionalized population with a disability estimate, and minority distributions (incl. African American, Hispanic). The selection criterion for these indices was the extent to which they holistically portrayed the personal economic and resilience landscape, as the majority of quantifiable disaster resilience is attributed to economic disposition (Ramezani & Farshchin, 2021).

However, the GRASP data is for 2020, not for 2050. To remedy this, Projections of the Total Population of Texas and Counties in Texas, 2020-2060 from the The Texas Demographic Center was utilized (You & Potter, 2022). Based upon a Cohort Component projection technique, these projections offer, per county, predictions for future populations while

factoring in aspects such as; fertility rates, baseline mortality rates, migration rates, and more. These predictions were used to extrapolate the 2020 GRASP vulnerability outputs to 2050.

Finally, economic evaluation of potential flood damages was carried out using data from the Global flood depth-damage function technical report, provided by the European Union (Huizinga et al., 2017). On the basis of extensive literature, construction cost surveys, and World Development Indicators, regional damage value functions for different land use classes were created.

### ***3.5 Data analysis method***

#### ***3.5.1 GIS analysis***

##### ***3.5.1.1 Data processing and Preparation***

The starting point of the project lay in the alteration of the existing topographical data in order to represent the effects of continued, unchanged, groundwater and natural resource extraction practices. Utilizing the network of historical data subsidence data, per the USGS, individual point trends were used in order to establish annual subsidence rates, which were subsequently applied and projected to model extents in 2050 (Ramage & Adams, 2022). The extrapolation of subsidence rates was a simple extension of the annual rate, multiplied to fill the gap between 2022, the most recent data year, and 2050, the target year.

Unfortunately, this data required further transformation prior to its introduction to the DEM, given the difference in continuous raster and point data. To remedy this, Triangulated Irregular Network (TIN) interpolation was selected, per best practice criterion for elevation-based interpolative techniques (Luedeling et al., 2007). The final 2050 subsidence interpolation range then combined with the 2021 DEM, utilizing the raster calculator, creating the final 2050 DEM.

##### ***3.5.1.2 Inundation Calculation and Validation***

With the projected 2050 DEM completed, the creation of the inundation extents was executed through altitude calculation and intersect analysis - utilizing sea level and storm surge extents and a novel coastline vector. Whereas sea level rise predictions are commonly accessible, per the IPCC reports, four varying RCP scenarios were selected in order to encompass the full variability of future outcomes - namely RCP 2.6, 4.0, 6.0, and 8.5, following similar research (Miller & Shirzaei, 2021). From this, the following SLR values were used; 0.25m, 0.26m,

0.26m, and 0.32m - respectively. Within the RCP scenarios, the values for 2050 for RCP4.0 and 6.0 are the same, and only diverge later in 2100.

The storm surge predictions, on the other hand, were extracted from Bass et al., 2018, simulating potential tropical cyclone intensities and sizes. The following values were extracted for use; 0.5m, 2m, 4m, and 8m (Miller & Shirzaei, 2021; Bass et al., 2018).

Using these values, inundation mapping practices were followed from the United Nations Platform for Space-based Information for Disaster Management and Emergency Response (UN-SPIDER). Employing the raster calculator function on the basis of the modified DEM - selection zones encompassing all areas below the hypothesized water levels were created (0.25m, 0.26m, and 0.32m for RCP SLR, and 0.5m, 2m, 4m, and 8m for storm surge extents). These predictions accounted for the varying RCP pathways, with the storm surge values having the relevant SLR values applied. However, these direct selections were an untrue representation of flood extents due to selection being exclusively altitude based, with inland areas with no water access being selected as well.

To remedy this, intersect analysis with a coastline file was required - with all selections not touching the coast or waterways larger than 10m being omitted - constrained by the DEM resolution of 10x10m pixels. This coastline vector was additionally created using the projected 2050 DEM and the raster calculator, creating a selection at sea level and including only connected features - with some manual correction to account for feature interruption such as bridges, or waterways being unclear in areas such as the wetlands.

Ultimately, these steps yielded inundation predictions across RCP and storm surge scenarios for 2050, while accounting for future subsidence-based topographical shifts. These predictions were then cross-referenced against sample inundation extent maps for different SLR scenarios by the NOAA to assess validity.

The manner in which this validity assessment was executed was through GIS and visual analysis. Naturally, given the significant difference in input quality, processing power, and processing approach, the NOAA file offered significantly higher resolution - allowing it advanced mapping of areas previously marked inaccessible to water due to the DEM resolution this research utilized.

For the GIS validation, Overlay Analysis was employed between novel 32cm and NOAA 30cm projections (nearest match). In this, two vectors can be overlaid, and percentage overlap is given. In this, the novel inundation extent was 78% of the NOAA file. Visual comparison revealed two key findings. To start, the NOAA extent included a larger area under its 30cm projection. However, the majority of the difference in extent was within the marshlands, whereas the 10x10m DEM resolution used for this research was unable to identify such narrow waterways. While this affects the summary statistics of inundation area, as these marshlands are not a land use of interest for further analysis within this paper, this is seen as an acceptable difference. Secondly, within the area of interest (the developed zone of the GHA) the faithfulness of the novel extent proved to be quite high - with few exceptions. Thus, the extent calculations were deemed sufficiently accurate given validation.

### ***3.5.2 Artificial Neural Network***

While the generated inundation extents, in their singular essence, may prove useful in simply demonstrating the varying areas at risk, their true strength lies in their overlay ability with various data layers - granting new insights. One of such layers is land use, a metric which offers critical urban information - particularly land value. In addition to this, data on inundation depth and land use type can be used in tandem to create an economic assessment of losses and damages - an invaluable tool for stakeholders in the cost-benefit discussion of resilience building and infrastructure planning.

The delphic nature of land use prediction is built on a complex system with roots more anthropogenic than binary. These predictions were carried out using the Artificial Neural Network (ANN) model, paired with Cellular Automata (CA). ANN models are the extreme simplification of human neural systems - composed of computational units analogous to that of the neurons of the biological nervous system - known as artificial neurons (Jeswal & Chakraverty, 2021). These networks are applied to assess the likelihood of land use transition using output neurons for simulating said changes (Figure 4).

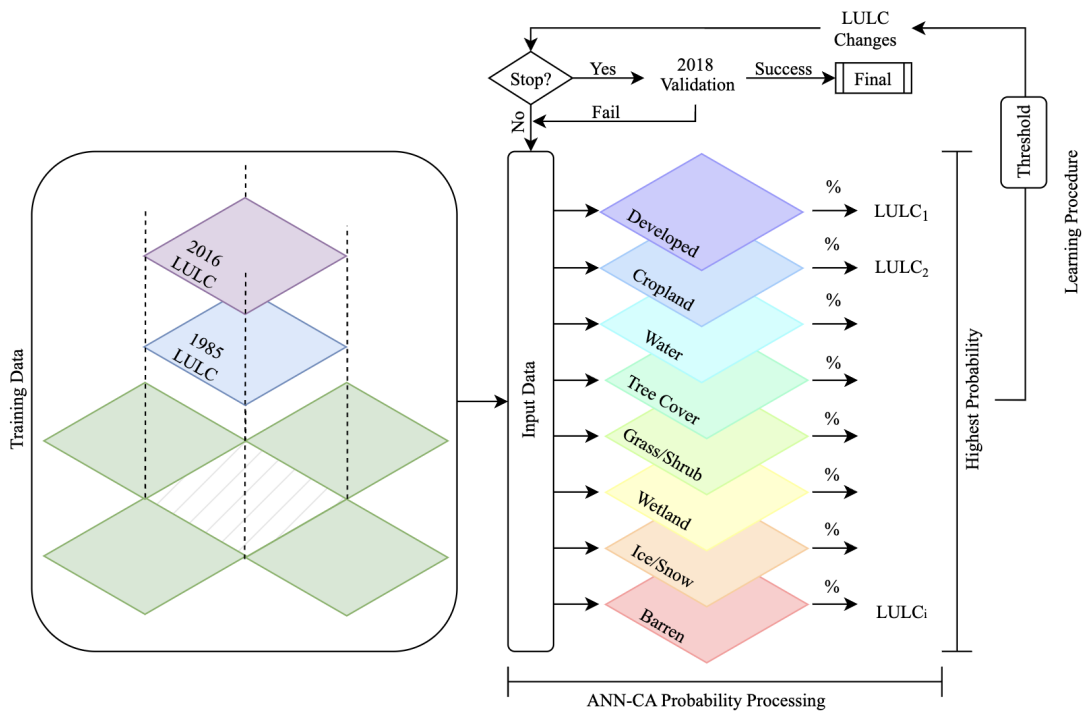


Figure 4. ANN-CA LULC Transition Model. Author made, adapted from Saputra & Lee, 2019

Within this network, each cell (pixel) can hold a multitude of values in which the model can assess transition, but for the purpose of this study, land use was the singular focus. In order to create the basis for training the model, a one-way raster analysis was executed across 1985 and 2016 land use rasters from the USGS LCMAP project. This resulting transition raster has 49 unique values, given the 7 land use types each raster contained, in addition to a transition matrix.

Upon this, the ANN-CA model is built on the functionality of the input, hidden, and output layers, wherein each spatial variable is associated with a neuron in the input layer. Within each model iteration, every artificial neuron generates a novel transition probability between two land uses, and continues to do so within an iterative framework. The manner of which this is done is through cellular automata, where the behavior of a cell is computed in relation to the nature of its neighbor and its future land use. Ultimately, land use change is determined through the assessment of all hypothetical transition values and selection of the highest (Saputra & Lee, 2019).

Prior to the generation of the desired snapshot of 2050, the newly trained model is validated using an existing land use raster - as the model was trained on 1985-2016, it was validated on

its ability to accurately predict 2018, the most recent snapshot provided by the LCMAP project. Once the kappa coefficient - the mathematical extent to which the predicted 2018 and actual 2018 land uses were similar - was sufficient, the model was tasked with the creation of the 2050 land use. The ultimate kappa within this research was at 81%, which is within acceptable range - per similar studies and instructional guides for the tool (Saputra & Lee, 2019).

### ***3.5.3 Social Vulnerability Index Based Vulnerability Assessment***

To translate these predictions from the physical to the human domain, the social vulnerability indices from the ATSDR's GRASP metrics were employed. These metrics were offered per census tract, though to simply include all tracts affected through the different inundation scenarios would offer a low degree of accuracy and differentiation between extents, due to tract size. In order to remedy this, a density raster conversion was required, in which the metric of interest was divided by the tract area and population, and scaled per 100m<sup>2</sup>, in order to create an output raster of 10x10m cells - matching the resolution of the inundation extents. These conversions were done using the field calculator, and then rasterised. Naturally, this approach is dependent on the assumption of equal distribution of people affected by the metric in question across the tract, which is not inherently true, but is a necessary assumption in order to proceed.

Upon the raster unique values output of this overlay, an estimation of denizens of the metric of interest affected per extent was generated. This was done through the multiplication of the pixel value by its count, and summed. Given the incredibly fine values this density conversion resulted in, a 10 digit significant figure delimitation was used for values to best prevent loss of accuracy. Upon this, a test sum of a density raster was compared against the full sum for validation purposes, resulting in a 99.994% accuracy rating.

However, the density sum function is limited to the number of people affected in the year of the GRASP file, 2020, whereas the predictions required are for 2050. To remedy this, Projections of the Total Population of Texas and Counties in Texas, 2020-2060 from the The Texas Demographic Center was utilized (You & Potter, 2022).

Wherein calculating the percentage change between 2020 and 2050, this rate of change was applied to the social vulnerability index inundation outputs - adjusting them to 2050 values -



again using the field calculator. Chambers is expected to undergo the biggest population increase of 51%, with Galveston and Harris expecting 32% and 22%, respectively - yielding a projected tri-county growth rate of 35% from 2020 to 2050, which was applied to the 2020 values. This 2020 to 2050 transformation is based on the assumption that factors affecting the social vulnerability indices remain constant within the interim period, which is untrue, but manual rate synthesis for trends within each metric falls beyond the scope of this study.

#### ***3.5.4 Economic Evaluation***

The process of economic valuation of the inundated extents was a simple process, on the basis of the North American values for Developed (averaging commerce, residential, and industrial values), and Cropland, from the EU Global flood depth-damage function report (Huizinga, De Moel, & Szewczyk, 2017). Averaged values for Developed are a necessity, given that at the resolution that the MOLUSCE land use model was able to provide, sub-distinctions across those three classes were not possible for this study. While content damage estimations were provided, given the variability of goods costs, and the already semi-dated values the report used, structural damage costs alone were selected due to price stability. This is particularly relevant, given the predictive nature of this research.

Extraction of depth-cost values from the functions provided, in the absence of a table, is an imprecise art. As such, a margin of error (MOE) will be factored into the values. Furthermore, as the EU functions only provide values to 6m of inundation, these values will be applied as the closest value available to the 8m surges modeled. This is done on the basis that the damage factor curve is at maximum at 6m, implying that economic losses are equivalent at, and beyond, the 6m point. Flood Damage-Depth curves can be found in Appendix B.

Lastly, as economic projections for costs for agriculture are only provided including the damages to warehouses and their contents for North America - significantly increasing the cost per m<sup>2</sup> in comparison to direct agricultural costs, an alternative method was employed. As per the EU Reports Appendix B: maximum damage in agriculture, the United States is listed at 416 USD per hectare (Huizinga, De Moel, & Szewczyk, 2017). Following the associated North American damage curve, wherein the maximum value of 1.0 at 6m is to be understood at 416 USD, then where the damage curve lies at 0.3 at 0.5m, costs can be assumed to be 30% of maximum - 124.8 USD per hectare, or 0.011 eur per m<sup>2</sup> (Appendix B;

Figure 4). The rest of the depth values for Agriculture are filled out similarly following this function.

The values used are as follows, with a MOE of  $\frac{1}{4}$  of the Y axis graduation to account for graph interpretation. For Agriculture, the MOE was  $\frac{1}{4}$  of the damage factor interval - 0.05 - multiplied by the maximum cost. As the inundation areas (Appendix B: Table 1) are ranges, the median values are applied to the cost function.

As per other studies, economic assessment of inundation is only carried out on the land uses of which have direct economic significance and value - namely agriculture and urban (Prahl et al., 2018; Smith, 1994). While this omits the inherent value of natural elements and their ecosystem services, the economic evaluation of these benefits and their resultant depth-cost curves are yet to be developed.

The economic assessment itself was carried out through creating altitude masks in 1m increments using the raster calculator, subsequent clipping of land use rasters to these masks, followed by a raster unique values report of the inundated areas, yielding the land uses and their areas. Through the omission of each following raster from the previous, descending in altitude, 1 meter land use increments were possible. In order to convert the area by altitude range to inundation depth, the values were inverted - to reflect the manner in which flood water depth decreases as the altitude increases within a flooded area. As an illustration of this, an area of which would undergo inundation at a 0.5 (0-1m) surge, would be under 8m+ of water in a 8m surge (with SLR applied) by 2050.

As such, the primary difference between the RCP 2.6 and 8.5 inundation extents lay in the 0-1m range, and was modeled thereafter. This is due to the 0-1m selection being the section in which the 10cm difference in SLR between the RCP's lay (8.25m vs 8.35m, respectively) lies, the 8m+ surge extent (0-1m flood depth) land uses are the only ones that differ in Table 3 (Appendix C). Finally, the land values from Appendix B: Table 1 are applied, yielding an economic prediction of incurred costs of flooding given 2050 land uses and sea level predictions.

It should be noted that this process of altitude partitioning invalidates the connectivity requirement for water to flood upon which the other projections were made. For example,

areas which would be inundated at 4m depth, within a 8m scenario, could otherwise have remained untouched, as connectivity was only possible through a higher water level. As such, the results of this analysis can only be considered valid within the context of the scenarios they offer (RCP2.6-8.0, 8m surge).

## 4. Results

### 4.1 Inundation results

Novel inundation extents were created on the basis of projected subsidence for 2050, in order to estimate the resultant flooding stemming from varying RCP SLR and storm surge predictions. The SLR, and SLR plus storm surge, projections are discussed below, with precise extents offered in Appendix C.

#### 4.1.1 Inundation maps under SLR of RCP2.6

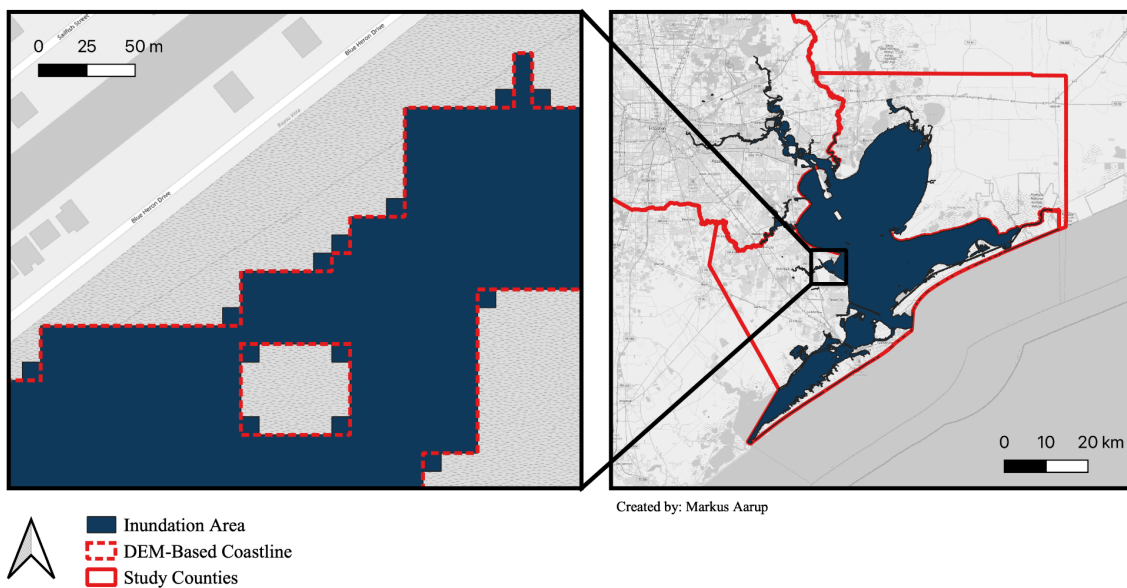


*Figure 5: Map of Projected Inundation of the Greater Houston Area in 2050, with RCP2.6 Sea Level Rise and Subsidence Predictions*

Within this map, inundation extents for the GHA are shown under a simulated 2050 scenario, wherein the RCP2.6 was followed for 0.25m increase in sea level, and subsidence projections are applied. Here, a coastal closeup of a semi-urbanised section near Texas City and San Leon - one of the more urbanized regions near the sea within the study area - is offered. In this, the pixels outside the original coastline (dashed line, red), represent 100m<sup>2</sup> areas which have succumbed to sea level rise driven inundation. In this scenario, the majority inundated land uses are as follows: Barren (80.05%), Grass/Shrub (9.08%), and Developed (5.74%).

### 4.1.2 Inundation maps under SLR of RCP 8.5

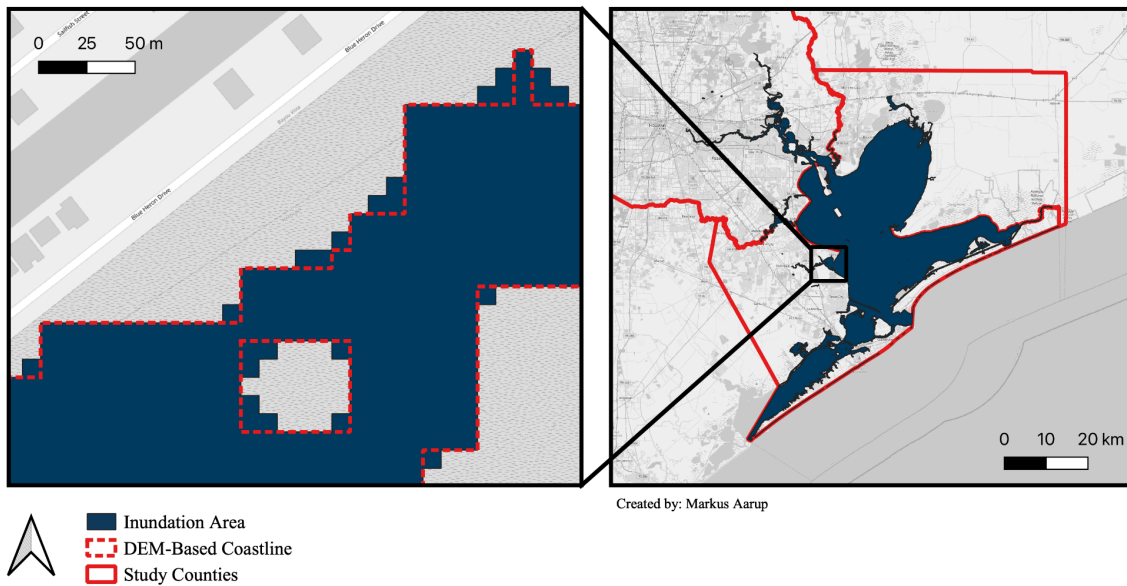


*Figure 6: Map of Projected Inundation of the Greater Houston Area in 2050, with RCP8.5 Sea Level Rise and Subsidence Predictions*

Within this map, inundation extents for the GHA are shown under a simulated 2050 scenario, wherein the RCP8.5 was followed for 0.32m increase in sea level, and subsidence projections are applied. In this scenario, the majority inundated land uses are as follows: Barren (77.75%), Grass/Shrub (10.96%), and Developed (5.85%).

### 4.1.3 Inundation area across RCP's for 2050

Under the lowest RCP scenario modeled, 0.25m SLR, 1,282,000m<sup>2</sup> will become inundated, whereas under the highest, 0.32m SLR, 1,459,000m<sup>2</sup>. The land use breakdown of the varying SLR extents can be found in Appendix C: Table 1 - note that water was omitted from proportion calculations to remove the influence of existing water (Galveston Bay and major tributaries) within the area.

Of interest within this distribution is the consistently high degree of 'barren' land which is inundated. As per USGS classification, barren is any land composed of "natural occurrences of soils, sand, or rocks where less than 10% of the area is vegetated.". This classification applies to sand, which would explain that the sandy coasts will be the most inundated under small flood extent changes.

#### 4.1.4 Inundation maps under SLR RCP 2.6, subsidence, and high storm surge

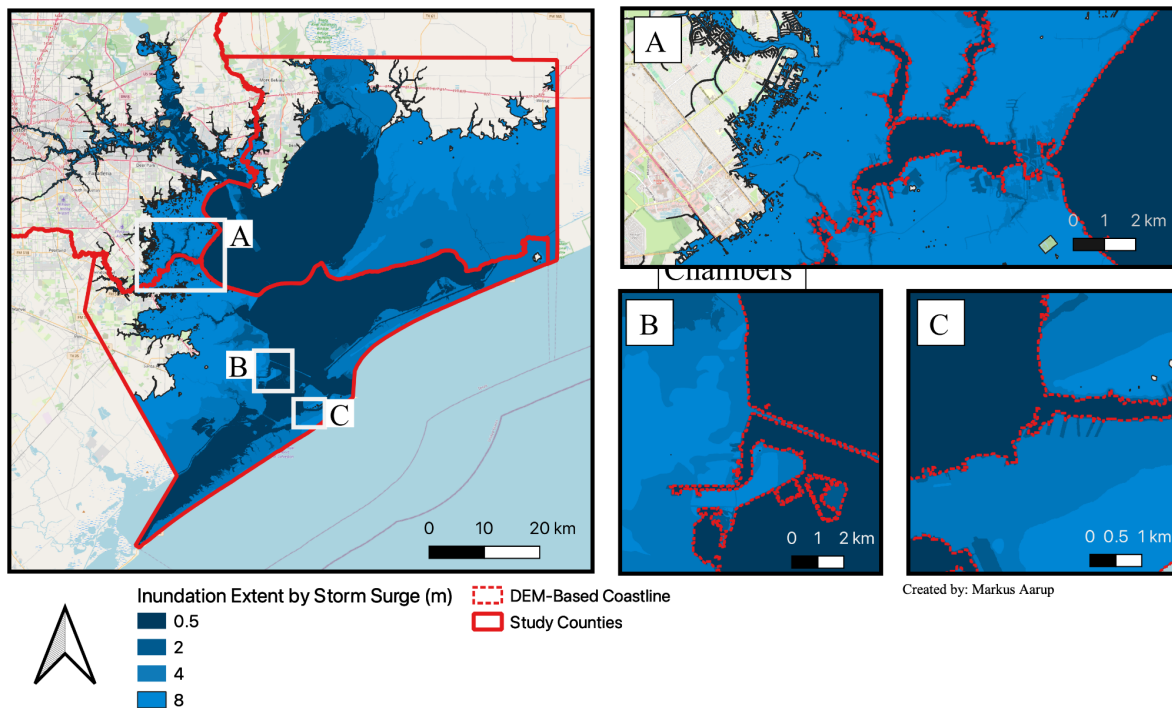


Figure 7: Map of Projected Inundation of the Greater Houston Area in 2050, with RCP2.6 Sea Level Rise, Subsidence, and Storm Surge Predictions. Highlighted: South Houston (A), Texas City (B), Galveston Island (C).

Figure 7 shows the expected inundation extents across the GHA for the year 2050, wherein future subsidence rates have been incorporated, in addition to the storm surge extents from Bass et al., (2019), on the basis of RCP2.6 sea level rise. In this, three snapshots of the areas of highest urban population have been included, namely; Houston, Texas City, and Galveston Island. Under 0.5m surge, the most prevalent inundated land uses are the following; Barren (76.09%), Grass/Shrub (11.23%), and Developed (6.39%). Under 8m surge, however, the most prevalent inundated are the following; Wetland (38.89%), Cropland (28.26%), and Developed (23.88%). Precise areas can be found in Appendix C: Table 2.

Particular attention should be paid to the particularly high inundation extent seen in the top right county, Chambers. Here, a large majority of the inland area becomes inundated between 2 & 4m storm surge - attributed to the majority of this county being either wetland or agriculture, and thus lacking the same infrastructure defenses or planning of urbanized areas. Exemplified by the decreased inundation extents in the top left county, Harris, wherein

Houston city is located. That said, the topography of the area is also more conducive to flood resilience, with Harris uniquely being situated upon an incline.

#### 4.1.5 Inundation maps under SLR RCP 8.5, subsidence, and high storm surge

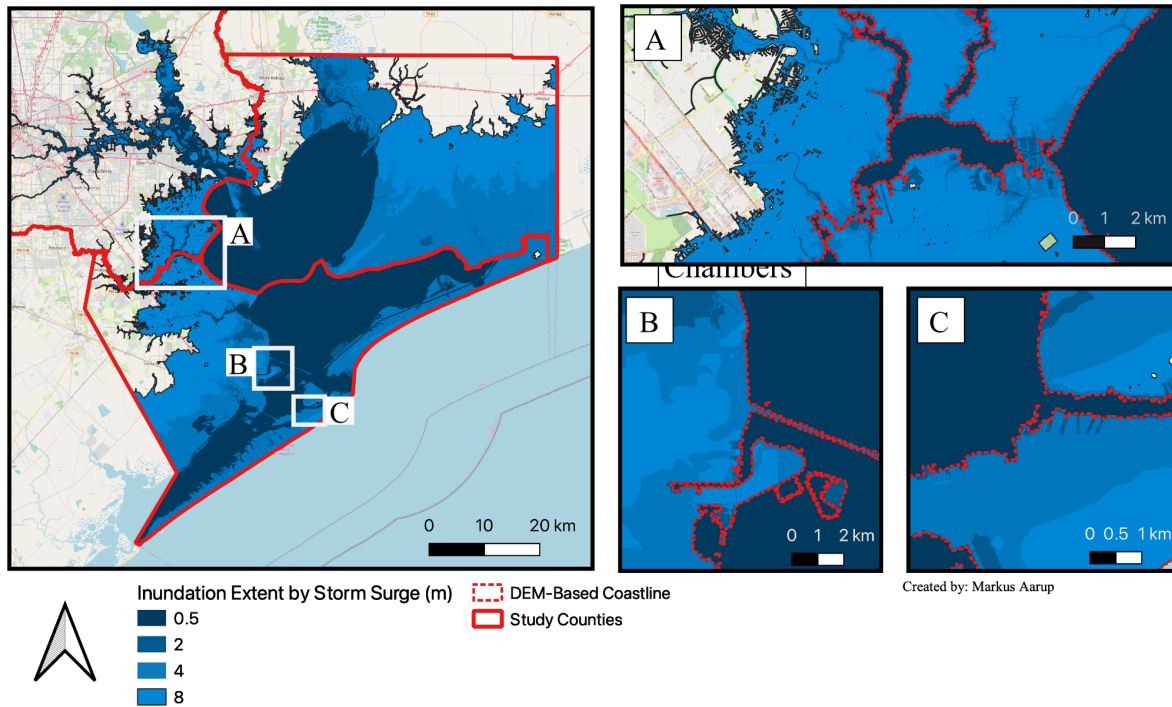


Figure 8: Map of Projected Inundation of the Greater Houston Area in 2050, with RCP8.5 Sea Level Rise, Subsidence, and Storm Surge Predictions. Highlighted: South Houston (A), Texas City (B), Galveston Island (C).

Figure 8 shows the same conditions as Fig.7, except with RCP8.5 sea level rise. Under 0.5m surge, the most prevalent inundated land uses are the following; Barren (75.99%), Grass/Shrub (11.21%), and Developed (6.32%). Under 8m surge, however, the most prevalent inundated are the following; Wetland (38.59%), Cropland (28.41%), and Developed (24.03%). Precise areas can be found in Appendix C: Table 2.

Given the minute ( $\pm 7\text{cm}$ ) variance between RCP SLR values, the homogenous trends between Figure 7 and 8 are to be expected. Similarly, the per-county inundation trends outlined in 4.1.4 hold for RCP8.5 projections. That said, there is still a difference of 21,376,000 m<sup>2</sup> between the 8m storm surge scenarios - attributed to the 7cm difference in base SLR. This only accounts for 1.03% between maximum inundation extents across RCP's at 8m.

#### 4.1.6 Inundation area across RCP's, subsidence, and storm surge for 2050

Within the storm surge scenarios, by 2050, the inundation extents range from 1,765,000 to 2,049,279,000 m<sup>2</sup> for RCP 2.6, and from 1,785,000 to 2,070,655,000m<sup>2</sup> for RCP 8.5, for 0.5 and 8m predictions respectively (Appendix C: Table 2). Across RCP's, Texas City and Galveston both remain relatively untouched within 0.5 and 2 meter surges, but suffer mass inundation post the 4m mark - as can be seen echoed in Appendix C: Table 2 with the Developed area increasing by over 100,000,000m<sup>2</sup>. However, Houston remains primarily undisturbed across all scenarios - owing to its significantly higher altitude than other developments within the bay area.

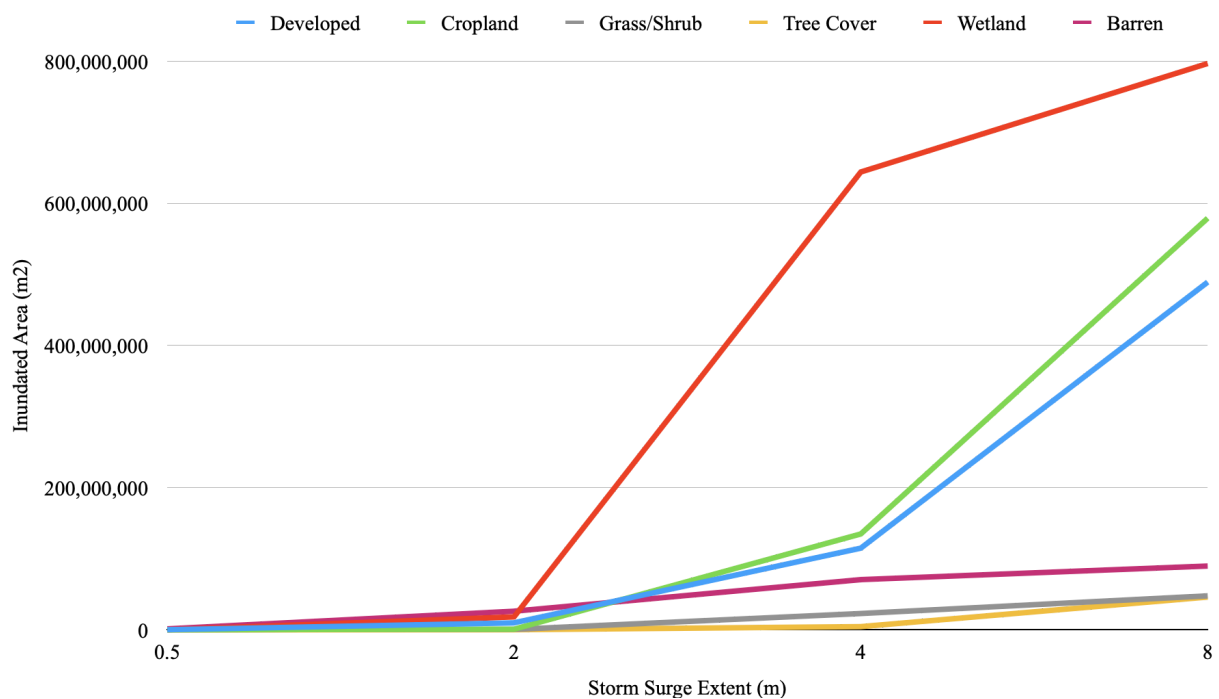


Figure 9: Trends in terms of inundation area across Land Use under different scenarios, with subsidence, RCP2.6 and 8.5 (Averaged)

Within the surge predictions, the following observations have been produced from Appendix C:Table 2 and Figure 9. To start, there is minor (proportional to the 8m surge extents) inundation up to the 2m surge mark. Following this, however, the inundation of wetlands significantly increases by 97% under 4m surge predictions. This is significantly higher than the rest of the land uses, though of additional note is cropland and developed both additionally take a sharp increase in flooded area, with barren, grass/shrub, and tree cover



showing little change. Finally, between the 4 and 8m storm surge extents, developed and cropland mirror the sharp increase wetlands did between 2 to 4m, with an increase of 77%.

These seemingly exponential trends are, of course, in part attributed to the surge extent iteratively increasing twofold. That said, the mass inundation of wetlands and cropland is a reasonable trend to expect, given the prevalence of utilizing floodplain flattened areas for agriculture, and wetlands already being partially inundated (Bremond et al., 2013). Important to note is the omission of existing flood infrastructure from calculations, due to their presence not being captured by the DEM resolution employed. However, with the Galveston Seawall (5.2m) and Texas City Levee (4.6-7m) only protecting specific areas and only to a certain point, the trends here are still applicable with Developed increasing significantly between 4 and 8m surge.

#### 4.2. Economic damage

Economic assessment of damages was done on the basis of three key inputs; the flood depth-damage values, the novel inundation extents, and future land uses. The results of the predictive land use model and the resultant economic projection is offered below.

##### 4.2.1 Projection of Land use change

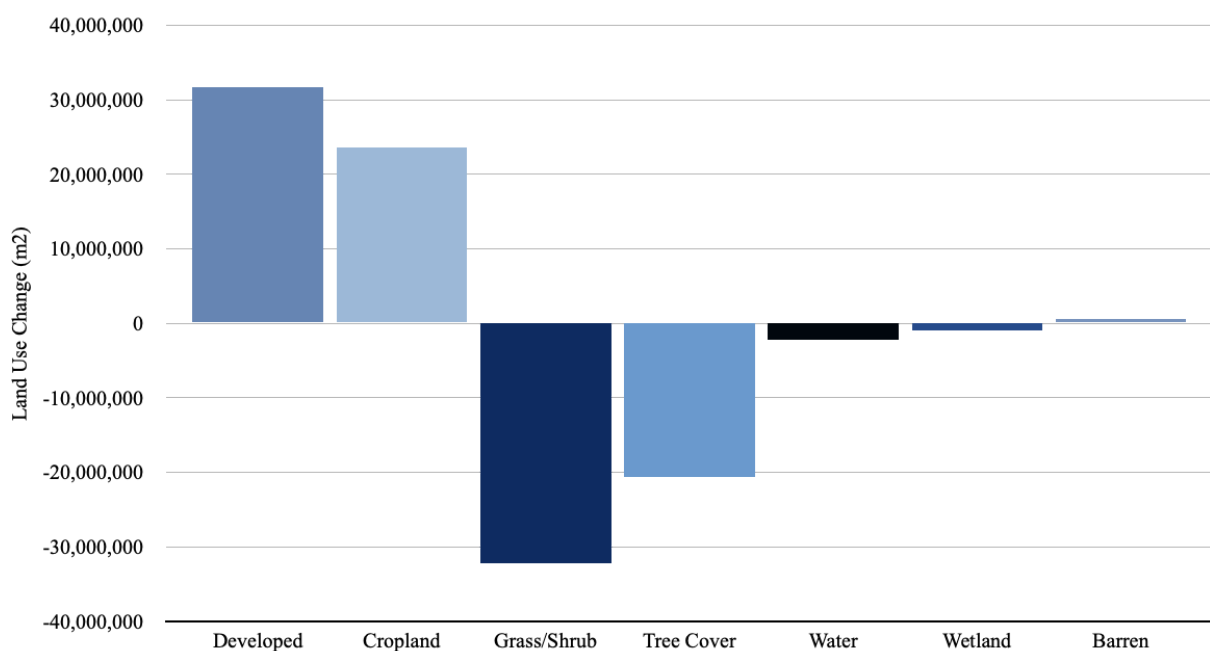


Figure 10: Predicted Land Use Change between 2020 and 2050, by Land Use.

Figure 10 outlines the change extents predicted by the MOLUSCE Land Use conversion projection (Appendix C: Table 5). In this, the primary land use conversions are as follows; Positive - Developed (+ 31,740,221 m<sup>2</sup>), Cropland (+ 23,660,467 m<sup>2</sup>), and Negative - Grass/Shrub (-32,155,443 m<sup>2</sup>), Tree Cover (-20,612,809 m<sup>2</sup>). Assessing these conversions, the predictive model posits that by 2050, significant areas which are currently vegetated (either with grass, shrubs, or trees) will become repurposed for anthropogenic purposes - either agriculture or urbanization. Here, the urbanization has spread as a buffer from existing development (Appendix C: Figure 10)

#### ***4.2.2 Potential Economic Damage (due to climate change and land use change)***

Assessment of potential incurred costs of inundation, when factoring in land use change, sea level rise, subsidence, and storm surge was done on the basis applying a depth-cost curve and values to the inundation extents outlined above. Precise values can be found in Appendix C: Table 4.

Here, an interesting relationship emerges. Proportionally, 0.5 exists to 8 in a ratio of 1:16. However, the predicted incurred costs lie at a ratio of 1:10,699, and 1:13,640 from 0.5m to 8m in surge (RCP2.6 and 8.5, respectively). This lack of direct ratio is explainable by; topography and land use. For a linear relationship, the area topography would require an even distribution of land use across a fixed slope, to allow the cost to increase directly with flood height. This relationship is more correctly encapsulated by the flood damage curve, in which an s-bend logarithmic curve shows that as depth increases, damage does so to a power above one - to a point upon which it plateaus.

This plateau is additionally part of the reason the 8m surge is radically beyond the point of linear understanding. In the EU curves utilized, maximum damage value is at 6m surge. Given the 8m surges in this research, this places a massive amount of land (366,490,000 m<sup>2</sup> developed, alone) around or above 6m - yielding incredibly high damage values (Appendix C: Table 3).

While the ultimate flood values for 8m inundation are immense, the threat that an 8m surge poses is not to be undersold. While parallel literature may not offer such extreme values -

which can largely be attributed to the resolution of the land use prediction for developed - important to note that these values are for an urban area with projected increased vulnerable area, thus literature and historical costs are undervalued.

#### ***4.3 Affected population under Storm Surge Minimum and Maximum Scenarios.***

Across RCP 2.6 - 0.5m, and RCP 8.5 - 8m, up to 120,000 people considered vulnerable by the ADSTR's GRASP framework are within projected inundation extents (Table 3). SVI inundation extent visualizations are provided in Appendix B: Figures 1-9, with population added for reference. Here, individuals may be multi-group, thus a total summary figure is not possible. Regardless, valuable conclusions stem from SVI impact assessments below, with further analysis offered in section 4.4.

When comparing the number of people within affected zones, it is essential to contextualize the figure in order to see if the people of each SVI is disproportionately being affected by the flood zone. In order to do this, a comparison of the proportion of total SVI in the affected area versus the total SVI in the study area is needed, against the population of the affected area versus the total population of the study area. In doing so, the following population proportion figures were created; 5% and 22% - meaning that 5% of the total population is located within the 0.5m inundation zone, at 22% within 8m.

As such, comparison of these figures against the SVI proportions in Table 3 yield unexpected findings. From literature, it would have been expected to see all the SVI proportions be higher than the population proportion - indicating a disproportionate impact. However, it would seem that only Unemployment and Disability are overrepresented in the inundation area - across scenarios (5.58% & 24.17%, and 6.97% & 25.93%, respectively). Conversely, the number of people below the 150% poverty line, those housing burdened, uninsured, and of minority status, are all underrepresented by up to 1.23% and 2.24%, for 0.5m and 8m respectively. Some research outlined in 2.5 did posit that ethnic factors were less dependent for disaster impact in the GHA, but rather elements such as education and income - which is mirrored in the unemployment SVI being disproportionately affected.

Table 2: Socially Vulnerable Peoples within Minimum and Maximum Inundation Storm Surge Extents, with Proportion of Total SVI (rounded to the nearest person)

Vulnerability Index	RCP 2.6 - 0.5m			RCP 8.5 - 8m		
	2020	2050	Affected Proportion (%)	2020	2050	Affected Proportion (%)
Poverty 150%	3,925	5,299	4.77	87,996	118,794	20.68
Unemployment	654	882	5.58	13,225	17,854	24.17
Housing Burdened	2,016	2,722	4.68	42,406	57,248	20.19
Uninsured	3,591	4,848	4.71	65,525	88,459	19.78
Disability	2,641	3565	6.97	53,971	72,861	25.93
Total Minority	9,270	12,514	3.77	205,438	277,341	19.76
African American	1,605	2,166	2.85	51,760	69,876	18.49
Hispanic	6,929	9,353	4.53	130,364	175,992	21.11

#### 4.4 Interpretation and Discussion

Whereas the results generally follow the logic outlined by the functional conceptual diagram outlined previously (Fig.2), there are some exceptions. The causal relationship between increased RCP and storm surge scenarios, and increased hazard, exposure, flood cost, and inundation extent were clearly seen in Figures 5-8. However, within vulnerability assessment - as touched on in 4.3 - the results do not follow the expected trends, warranting further investigation. Some papers, such as Mazmuder et al., (2021), Smiley (2020), and Brody et al., (2018), had found similar results disputing the expected trends of SVI and flood vulnerability. Smiley (2020) highlights that racial inequality particularly affects risk from impacts outside the direct flood range, meaning that the theoretical basis of this research may still hold, but lie outside the scope of the predictions done. In these works, locational aspects were highlighted as the key explanatory variable in assessing flood risk. However, residential distribution is deeply intertwined with racial factors.

Visual analysis of the SVI maps (Appendix B: Figures 1-9) offers some insights into the distributions of the SVI populations, and causal relationships can be extrapolated. Here, the relationship between minority status and socioeconomics is of the most interest, given the residential influence. Through map analysis and research, a potential explanatory variable that shaped the development of modern Houston became apparent - redlining.

Redlining was a discriminatory housing practice that was implemented in the United States, and specifically Houston, in the 1930's, involving the denial of loans, insurance, and other financial services to minority neighborhoods. Under HOLC demarcation, African-American neighborhoods were almost always designated as unsafe, denying them financial support for loans or insurance (Rothstein, 2017). Within the study area, and the GHA, for 2050, the corollary between African-American census tract density and those uninsured is high (Appendix C: Fig.5,8).

Areas that were previously redlined have increased rates of poverty, crime, and lack access to quality infrastructure (Sugrue, 2014). Historically redlined communities place over 60% higher than those unaffected in national vulnerability - assessed through parallel SVI's from GRASP (Nelson & Ayers, n.d.). This research, results seen in Figure 11, is of particular note in comparison with the resultant SVI distributions, wherein the singular green zone is often fully omitted from SVI densities in current and future projections. Further of interest is the left-distribution of HOLC unapproved areas and resultantly high SVI issues in the flood region of the river (highlighted in red). HOLC demarcation has affected the modern distribution of minorities within the GHA.

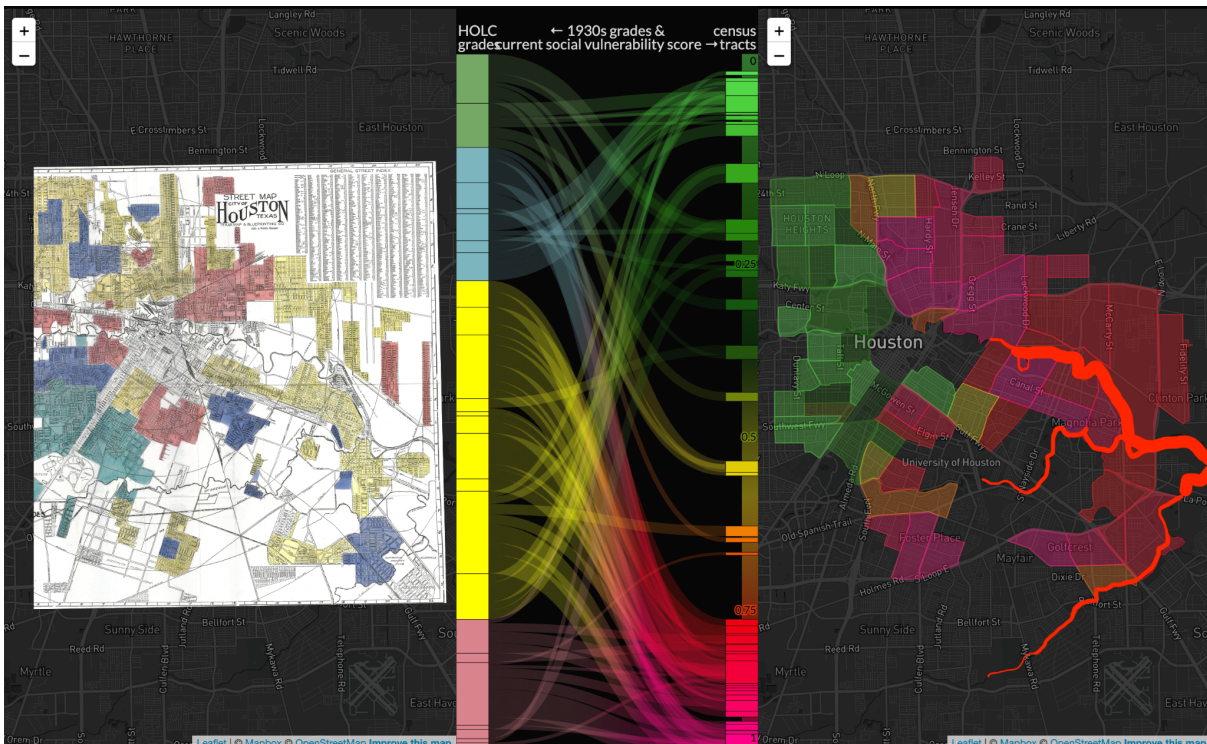


*Figure 11: The transition of historical HOLC ratings and current summary SVI ratings. Color code on the left indicates HOLC rating, with red being Hazardous and green Best, and on the right, pink being the highest prevalence of SVI issues, and green the lowest. (Nelson & Ayers, n.d)*

The effects of redlining are still felt by Black communities in Houston, and they will continue to be felt for generations to come. As exemplified by a relationship between minority status and being burdened by housing costs - a direct impact of being denied generational housing opportunity (Appendix C: Fig. 7,4). However, while this relationship is clear in the GHA, within the inundation area, the relationship is uncertain enough that it could be attributed to population density being a confounding factor (Appendix C: Figure 1). As redlining predominantly affected central Houston - an area outside the inundation extents - the results variance from literature trends could be attributed to this. Additionally, these are areas that would suffer under storm scenarios, but happen to fall outside inundation range - supported by Smiley (2020).

These redlining effects are compounded by current processes, such as gentrification. Coastal gentrification may be a driver as to why SVI populations within the affected surge zones may not follow the literature guided assumptions.

With climate change causing extremification of inland climates, regionally and locally - urban heat island effect - people are driven to relocate to milder coastal areas. Such an influx disrupts property values, displacing lower income residents who's original at-risk coastal settlement could be attributed to the HOLC (Caffyn & Jobbins, 2003). Furthermore, areas with increased flood risk see high rates of out-migration, opening it up to 'climate gentrification' (De Koning & Filatova, 2020). This works in parallel with 'resilience gentrification', wherein low-income groups affected by flooding lack financial means to rebuild, creating attractive low-cost property (Gould & Lewis, 2021). Additionally, Galveston Bay is a popular retirement location within the South, causing a high influx of settlers of disparate social and economic standing, exacerbating gentrification (Block, 2017). Of note is how Disability being overrepresented in the sample area supports the gentrification theory, as an influx of aging populations would increase this proportion.

Thus, while some patterns can be explained through historical analysis of Redlining, the discrepancies seen from literature can be attributed to modern social processes.

## **5. Conclusion**

This study aimed to assess the social and economic implications of flooding of the GHA in 2050, considering factors such as changing land uses, SLR and storm surge predictions, and population adjustment. Using numerous projections and transformations, the research generated findings to address the gap in predicted coastal flood research of the US, wherein social aspects are often omitted in favor of environmental and economic factors. The latter was additionally covered in this study.

Answering the primary research question requires addressing its constituent questions. Sub-question 1, a methodological issue, has been assuaged through the numerous varying GIS-based approaches (section 3.5) taken in order to create results that best answer the primary question. Ranging from artificial neural networks to TIN, each is crucial in adding a layer to the simulated GHA of 2050. Through these methods, 1.a. can be answered across numerous inundation scenarios of storm surge and RCP's (Figures 5-8, Appendix C: Tables 1,2,3). Sub-question 2 addresses the issue of cost enumeration, which has been answered through sections 3.5.4, 4.2.2, Appendix B: Table 1, and Appendix C: Table 4. These sections address potential flood costs, broken down by method, application, result, and trend. Finally, sub-question 3 covers estimation of socially vulnerable peoples affected - answered through sections 3.5.3, 4.3, Table 3, and Figures 1-9 (Appendix C). The holistic consideration of these sub-questions and their answers allow for answering of the Primary Research Question.

Under varying storm surge scenarios, by 2050, the inundation extents range from 1,765,000 to 2,049,279,000 m<sup>2</sup> for RCP 2.6, and from 1,785,000 to 2,070,655,000m<sup>2</sup> for RCP 8.5, for 0.5 and 8m predictions, respectively. These flood extents can cause between 17.6 million to 188 billion euro in damages for RCP 2.6, and 17.8 million to 242 billion damages ( $\pm$  10.3%) for RCP 8.5. Under these surge scenarios, up to 12.5k vulnerable peoples will be affected for RCP 2.6 0.5m, a minimum scenario, and up to 277.3k for RCP 8.5 at 8m, a maximum scenario. Upon review of these figures, the final answer to this is that the GHA is at high risk under future SLR and storm surge scenarios.

With results in mind, critically assessing methodology, and considering the suggestions in 2.6.1, the following suggestions were created for counties comprising the GHA:



- As per 2.6.1-1, the introduction of a climate-forward development framework with concrete goals and plans. Currently, the 2023 Houston climate plan, within buildings, is simply focused on materials and insulation for cost saving measures. Given the lack of centralized development planning to enforce policy, economic incentives such as tax breaks could be considered for developers.
- As per 2.6.1-2, introducing further equitable development regulations and incentives. In a developer-led urban climate, low-income low-profit developments are low-priority. Currently there is a 9% tax cut available, but it faces issues of competition and accessibility. A 4% plan has been proposed, but clearly there is a need for more such soft-measure incentives.
- As per 2.6.1-4, increasing inclusivity in disaster and urban planning. While the inundated area demographic analysis did not reveal the trends expected, analysis of the GHA shows clear signs of historical inequality. Within a 8m storm surge, factors such as rainfall and infrastructure outside the flood extent will be important. This aligns with Houston's 2023 climate plan, goals 4-7, ensuring equitable neighborhoods.
- As per 2.6.1-6, further physical infrastructure developments can be planned on the basis of this research. Projects such as a barrier island sea spine would reduce the bay's flood intake, and management of ecosystem services (such as preventing the predicted mass transition from grass/shrubs/trees to urban/agriculture) would safeguard the area's natural flood resiliency. This aligns with Houston's Climate plan, goals 7,8,16. The potential incurred flood costs and the damage-depth ratio outlined could be used for cost-benefit proposals for infrastructure.

Beyond these suggestions, there are a number of recommendations to be had for future research, beyond the research gaps identified in 2.7, which would address certain limitations of this research.

- Introduction of an advanced hydrological model for future planning. Altitude-based GIS is a strong indicator, but it remains a starting point for research. Omitting above mentioned features such as weather events and infrastructure, hydrological modeling would offer higher resolution information to plan with. Furthermore, inclusion of weather would introduce risk as a vector of analysis, which is important when contextualizing urban vulnerability.
- Increasing the training data of the predictive land use model would offer better understanding of trends and patterns, improving the accuracy of the forecasts. While

using 1985-2016 still yielded very reasonable development patterns, the majority of Houston's development predates 1985.

Thus, despite Houston's imminent threats, a combination of further research, infrastructure, and policy can shift the trajectory towards an equitable and safe future for all.

## ***Bibliography***

- Ansari, A., & Golabi, M. H. (2019). Prediction of spatial land use changes based on LCM in a GIS environment for Desert Wetlands—A case study: Meighan Wetland, Iran. *International soil and water conservation research*, 7(1), 64-70.
- Balica, S. F., Douben, N., & Wright, N. G. (2009). Flood vulnerability indices at varying spatial scales. *Water science and Technology*, 60(10), 2571-2580.
- Barros, M. T., Brandão, J. L., Silva, O. F., & Ono, S. (2005). The impact of urban sprawl on Flood Risk Areas. *Managing Watersheds for Human and Natural Impacts*. [https://doi.org/10.1061/40763\(178\)105](https://doi.org/10.1061/40763(178)105)
- Bass, B., Torres, J. M., Irza, J. N., Proft, J., Sebastian, A., Dawson, C., & Bedient, P. (2018). Surge dynamics across a complex bay coastline, Galveston Bay, TX. *Coastal Engineering*, 138, 165-183.
- Beevers, L., Walker, G., & Strathie, A. (2016). A systems approach to flood vulnerability. *Civil engineering and environmental systems*, 33(3), 199-213.
- Block, S. (2017, July 4). Why Galveston, Texas, is a great place to retire. *Kiplinger.com*.  
<https://www.kiplinger.com/article/retirement/t006-c000-s002-why-galveston-texas-is-a-great-place-to-retire.html>
- Bodenreider, C., Wright, L., Barr, O., Xu, K., & Wilson, S. (2019). Assessment of social, economic, and geographic vulnerability pre-and post-Hurricane Harvey in Houston, Texas. *Environmental Justice*, 12(4), 182-193.
- Bremond, P., Grelot, F., & Agenais, A. L. (2013). Economic evaluation of flood damage to agriculture—review and analysis of existing methods. *Natural Hazards and Earth System Sciences*, 13(10), 2493-2512.
- Brody, S. D., Sebastian, A., Blessing, R., & Bedient, P. B. (2018). Case study results from southeast Houston, Texas: identifying the impacts of residential location on flood risk and loss. *Journal of Flood Risk Management*, 11, S110-S120.
- Brody, S. D., Zahran, S., Highfield, W. E., Grover, H., & Vedlitz, A. (2008). Identifying the impact of the built environment on flood damage in Texas. *Disasters*, 32(1), 1-18.
- Buckley, S. M., Rosen, P. A., Hensley, S., & Tapley, B. D. (2003). Land subsidence in Houston, Texas, measured by radar interferometry and constrained by extensometers. *Journal of geophysical research: solid earth*, 108(B11).

- Caffyn, A., & Jobbins, G. (2003). Governance capacity and stakeholder interactions in the development and management of coastal tourism: Examples from Morocco and Tunisia. *Journal of sustainable Tourism*, 11(2-3), 224-245.
- Cea, L., & Costabile, P. (2022). Flood risk in urban areas: modelling, management and adaptation to climate change. A review. *Hydrology*, 9(3), 50.
- Center for Disease Control and Prevention/ Agency for Toxic Substances and Disease Registry/ Geospatial Research, Analysis, and Services Program. CDC/ATSDR Social Vulnerability Index [2020] Database [Texas].
- Chakraborty, J., Collins, T. W., & Grineski, S. E. (2019). Exploring the environmental justice implications of Hurricane Harvey flooding in Greater Houston, Texas. *American journal of public health*, 109(2), 244-250.
- Chan, S. W., Abid, S. K., Sulaiman, N., Nazir, U., & Azam, K. (2022). A systematic review of the flood vulnerability using geographic information systems. *Heliyon*.
- Chen, J., Hill, A. A., & Urbano, L. D. (2009). A GIS-based model for urban flood inundation. *Journal of Hydrology*, 373(1-2), 184-192.
- Collins, T. W., Grineski, S. E., & Chakraborty, J. (2018). Environmental injustice and flood risk: a conceptual model and case comparison of metropolitan Miami and Houston, USA. *Regional environmental change*, 18, 311-323.
- Collins, T. W., Grineski, S. E., Chakraborty, J., & Flores, A. B. (2019). Environmental injustice and Hurricane Harvey: A household-level study of socially disparate flood exposures in Greater Houston, Texas, USA. *Environmental research*, 179, 108772.
- Comptroller Texas. (2022). The Gulf Coast REGION2022 Regional Report. The Gulf Coast Region. <https://comptroller.texas.gov/economy/economic-data/regions/2022/gulf-coast.php>
- Davlasheridze, M., Atoba, K. O., Brody, S., Highfield, W., Merrell, W., Ebersole, B., ... & Gilmer, R. W. (2019). Economic impacts of storm surge and the cost-benefit analysis of a coastal spine as the surge mitigation strategy in Houston-Galveston area in the USA. *Mitigation and Adaptation Strategies for Global Change*, 24, 329-354.
- De Koning, K., & Filatova, T. (2020). Repetitive floods intensify outmigration and climate gentrification in coastal cities. *Environmental research letters*, 15(3), 034008.

- Drane, A. (2023, January 24). Texas made record-shattering \$24.7B off oil and gas last year. *Houston Chronicle*.  
<https://www.houstonchronicle.com/business/energy/article/oil-gas-taxes-new-record-17736663.php>
- EPA. (2022, December 13). Climate Change and the Health of Socially Vulnerable People. Retrieved March 21, 2023, from <https://www.epa.gov/climateimpacts/climate-change-and-health-socially-vulnerable-people>
- Galloway, D. L., Coplin, L. S., & Ingebritsen, S. E. (2003). Effects of land subsidence in the greater Houston area. *Managing urban water supply*, 187-203.
- Gould, K. A., & Lewis, T. L. (2021). Resilience gentrification: environmental privilege in an age of coastal climate disasters. *Frontiers in Sustainable Cities*, 3, 687670.
- Griggs, G., & Reguero, B. G. (2021). Coastal adaptation to climate change and sea-level rise. *Water*, 13(16), 2151.
- Gulf Coast Aquifer subsidence. USGS. (2020). Retrieved March 2, 2023, from [https://txpub.usgs.gov/houston\\_subsidence/](https://txpub.usgs.gov/houston_subsidence/)
- Henson, M. S. (2020, November 9). Harris County. Texas State Historical Association. <https://www.tshaonline.org/handbook/entries/harris-county>
- Hicks, T., & Shamberger, K. (2023, February 7). Hurricane Harvey more than doubled the acidity of Texas' Galveston Bay, threatening oyster reefs. *Hurricane Harvey More Than Doubled The Acidity Of Texas' Galveston Bay, Threatening Oyster Reefs*.  
<https://artsci.tamu.edu/news/2023/02/hurricane-harvey-more-than-doubled-the-acidity-of-texas-galveston-bay-threatening-oyster-reefs.html>
- Houston Facts and figures. About Houston . (2023). Retrieved March 2, 2023, from <https://www.houstontx.gov/about/houston/houstonfacts.html>
- Huizinga, J., De Moel, H. and Szewczyk, W., Global flood depth-damage functions: Methodology and the database with guidelines, EUR 28552 EN, Publications Office of the European Union, Luxembourg, 2017, ISBN 978-92-79-67781-6, doi:10.2760/16510, JRC105688.
- IPCC, 2021: Summary for Policymakers. In: *Climate Change 2021: The Physical Science Basis*. Contribution of Working Group I to the Sixth Assessment Report of the Intergovernmental Panel on Climate Change [Masson-Delmotte, V., P. Zhai, A. Pirani, S.L. Connors, C. Péan, S. Berger, N. Caud, Y. Chen, L. Goldfarb, M.I.

- Gomis, M. Huang, K. Leitzell, E. Lonnoy, J.B.R. Matthews, T.K. Maycock, T. Waterfield, O. Yelekçi, R. Yu, and B. Zhou (eds.)]. In Press.
- Islam, K., Rahman, M. F., & Jashimuddin, M. (2018). Modeling land use change using cellular automata and artificial neural network: The case of Chunati Wildlife Sanctuary, Bangladesh. *Ecological indicators*, 88, 439-453.
- Jeswal, S. K., & Chakraverty, S. (2021). Fuzzy eigenvalue problems of structural dynamics using ANN. In *New Paradigms in Computational Modeling and Its Applications* (pp. 145-161). Academic Press.
- Ji, J., Choi, C., Yu, M., & Yi, J. (2012). Comparison of a data-driven model and a physical model for flood forecasting. *WIT Transactions on Ecology and the Environment*, 159, 133-142.
- Kamaraj, M., & Rangarajan, S. (2022). Predicting the future land use and land cover changes for Bhavani basin, Tamil Nadu, India, using QGIS MOLUSCE plugin. *Environmental Science and Pollution Research*, 29(57), 86337-86348.
- Kaźmierczak, A., & Cavan, G. (2011). Surface water flooding risk to urban communities: Analysis of vulnerability, hazard and exposure. *Landscape and urban planning*, 103(2), 185-197.
- Kia, M. B., Pirasteh, S., Pradhan, B., Mahmud, A. R., Sulaiman, W. N. A., & Moradi, A. (2012). An artificial neural network model for flood simulation using GIS: Johor River Basin, Malaysia. *Environmental earth sciences*, 67, 251-264.
- Kim, Y., & Newman, G. (2019). Climate change preparedness: Comparing future urban growth and flood risk in Amsterdam and Houston. *Sustainability*, 11(4), 1048. <https://doi.org/10.3390/su11041048>
- Kleiner, D J. (2021, April 7). Galveston County. Texas State Historical Association. <https://www.tshaonline.org/handbook/entries/galveston-county>
- Kleiner, D. J. (2020, October 8). Chambers county. Texas State Historical Association. <https://www.tshaonline.org/handbook/entries/chambers-county>
- Kok, S., Costa, A.L. Framework for economic cost assessment of land subsidence. *Nat Hazards* 106, 1931–1949 (2021). <https://doi.org/10.1007/s11069-021-04520-3>
- Lieberman-cribbin, W., Schwartz, R., & Taioli, E. (2019). Socioeconomic disparities in incidents at toxic sites during Hurricane Harvey. *Environmental Epidemiology*, 3, 239. <https://doi.org/10.1097/01.ee9.0000608504.45519.77>
- Lindsey, R. (2022). Climate change: Global sea level. NOAA Climate.gov. Retrieved March 2, 2023, from

<https://www.climate.gov/news-features/understanding-climate/climate-change-global-sea-level#:~:text=Global%20average%20sea%20level%20has,3.8%20inches%20above%201993%20levels>

- Liu, Y., & Chen, J. (2021). Future global socioeconomic risk to droughts based on estimates of hazard, exposure, and vulnerability in a changing climate. *Science of the total environment*, 751, 142159.
- Luedeling, E., Siebert, S., & Buerkert, A. (2007). Filling the voids in the SRTM elevation model—A TIN-based delta surface approach. *ISPRS Journal of Photogrammetry and Remote Sensing*, 62(4), 283-294.
- Maier, N., & Dietrich, J. (2016). Using SWAT for strategic planning of basin scale irrigation control policies: a case study from a humid region in northern Germany. *Water Resources Management*, 30, 3285-3298.
- Mazumder, L. T., Landry, S., & Alsharif, K. (2022). Coastal cities in the Southern US floodplains: An evaluation of environmental equity of flood hazards and social vulnerabilities. *Applied geography*, 138, 102627.
- Merz, B., Kreibich, H., Schwarze, R., and Thieken, A.: Review article "Assessment of economic flood damage", *Nat. Hazards Earth Syst. Sci.*, 10, 1697–1724, <https://doi.org/10.5194/nhess-10-1697-2010>, 2010.
- Messner, F., & Meyer, V. (2006). Flood damage, vulnerability and risk perception—challenges for flood damage research. In *Flood risk management: hazards, vulnerability and mitigation measures* (pp. 149-167). Dordrecht: Springer Netherlands.
- Miller, M. M., & Shirzaei, M. (2021). Assessment of future flood hazards for southeastern Texas: Synthesizing subsidence, sea-level rise, and storm surge scenarios. *Geophysical Research Letters*, 48, e2021GL092544. <https://doi.org/10.1029/2021GL092544>
- MohanRajan, S. N., Loganathan, A., & Manoharan, P. (2020). Survey on Land Use/Land Cover (LU/LC) change analysis in remote sensing and GIS environment: Techniques and Challenges. *Environmental Science and Pollution Research*, 27, 29900-29926.
- Muhammad, R., Zhang, W., Abbas, Z., Guo, F., & Gwiazdzinski, L. (2022). Spatiotemporal change analysis and prediction of future land use and land cover changes using QGIS MOLUSCE plugin and remote sensing big data: a case study of Linyi, China. *Land*, 11(3), 419.

- Nasiri, H., Mohd Yusof, M.J. & Mohammad Ali, T.A. An overview to flood vulnerability assessment methods. *Sustain. Water Resour. Manag.* 2, 331–336 (2016). <https://doi.org/10.1007/s40899-016-0051-x>
- Nelson , R. K., & Ayers, E. L. (n.d.). Not even past: Social vulnerability and the legacy of Redlining. *Not Even Past: Social Vulnerability and the Legacy of Redlining.* <https://dsl.richmond.edu/socialvulnerability/>
- Nielsen-Gammon, J., Escobedo, J., Ott, C., Dedrick, J., & Van Fleet, A. (2020). (publication). ASSESSMENT of HISTORIC and FUTURE TRENDS of EXTREME WEATHER IN TEXAS, 1900-2036.
- Office for Coastal Management, 2022: NOAA Digital Coast Sea Level Rise and Coastal Flooding Impacts Viewer. NOAA National Centers for Environmental Information, <https://www.fisheries.noaa.gov/inport/item/48241>.
- Opolot, E. (2013). Application of remote sensing and geographical information systems in flood management: a review.
- Oppenheimer, M., B.C. Glavovic , J. Hinkel, R. van de Wal, A.K. Magnan, A. Abd-Elgawad, R. Cai, M. Cifuentes-Jara, R.M. DeConto, T. Ghosh, J. Hay, F. Isla, B. Marzeion, B. Meyssignac, and Z. Sebesvari, 2019: Sea Level Rise and Implications for Low-Lying Islands, Coasts and Communities. In: IPCC Special Report on the Ocean and Cryosphere in a Changing Climate [H.-O. Pörtner, D.C. Roberts, V. Masson-Delmotte, P. Zhai, M. Tignor, E. Poloczanska, K. Mintenbeck, A. Alegría, M. Nicolai, A. Okem, J. Petzold, B. Rama, N.M. Weyer (eds.)]. Cambridge University Press, Cambridge, UK and New York, NY, USA, pp. 321-445. <https://doi.org/10.1017/9781009157964.006>.
- Pengra, B.W., Stehman, S.V., Horton, J.A., and Wellington, D.F., 2021, Land Change Monitoring, Assessment, and Projection (LCMAP) Collection 1.2 Annual Land Cover and Land Cover Change Validation Tables (1985–2018) for the Conterminous United States: U.S. Geological Survey data release, <https://doi.org/10.5066/P9M6T45Z>.
- Prahl, B. F., Boettle, M., Costa, L., Kropp, J. P., & Rybski, D. (2018). Damage and protection cost curves for coastal floods within the 600 largest European cities. *Scientific data*, 5(1), 1-18.
- Pulcinella, J. A., Winguth, A. M., Allen, D. J., & Dasa Gangadhar, N. (2019). Analysis of flood vulnerability and transit availability with a changing climate in Harris County, Texas. *Transportation research record*, 2673(6), 258-266.



- QGIS Python Plugins Repository MOLUSCE. Molusce - QGIS Python plugins repository. (n.d.). Retrieved March 2, 2023, from <https://plugins.qgis.org/plugins/molusce/>
- Quagliolo, C., Roebeling, P., Matos, F., Pezzoli, A., & Comino, E. (2023). Pluvial flood adaptation using nature-based solutions: An integrated biophysical-economic assessment. *Science of The Total Environment*, 166202.
- Ramage, J.K., and Adams, A.C., 2022, Cumulative Compaction (from Site Activation Through 2021) of Subsurface Sediments in the Chicot and Evangeline Aquifers in the Greater Houston Area, Texas (ver. 4.0, November 2022): U.S. Geological Survey data release, <https://doi.org/10.5066/P9YGUE2V>.
- Ramezani, R., & Farshchin, A. (2021). Urban Resilience and Its Relationship with Urban Poverty. *Journal of Urban Planning and Development*, 147(4), 05021042.
- Recommended practice: Exposure mapping. UN. (n.d.). Retrieved March 2, 2023, from <https://www.un-spider.org/advisory-support/recommended-practices/recommended-practice-exposure-mapping>
- Recommended practice: Use of digital elevation data for storm surge coastal flood modelling. UN. (n.d.). Retrieved March 2, 2023, from <https://www.un-spider.org/advisory-support/recommended-practices/recommended-practice-use-digital-elevation-data-storm-surge>
- Rehman, S., Sahana, M., Hong, H., Sajjad, H., & Ahmed, B. B. (2019). A systematic review on approaches and methods used for flood vulnerability assessment: Framework for future research. *Natural Hazards*, 96, 975-998.
- Rentschler, J., Salhab, M. & Jafino, B.A. Flood exposure and poverty in 188 countries. *Nat Commun* 13, 3527 (2022). <https://doi.org/10.1038/s41467-022-30727-4>
- Romali, N. S., Sulaiman, M. S. A. K., Yusop, Z., & Ismail, Z. (2015). Flood damage assessment: A review of flood stage–damage function curve. In *ISFRAM 2014: Proceedings of the International Symposium on Flood Research and Management* (pp. 147-159). Springer Singapore.
- Rothstein, R. (2017). *The color of law: A forgotten history of how our government segregated America*. Liveright Publishing.
- Saputra, M. H., & Lee, H. S. (2019). Prediction of land use and land cover changes for north sumatra, indonesia, using an artificial-neural-network-based cellular automaton. *Sustainability*, 11(11), 3024.

- Seenath, A., Wilson, M., & Miller, K. (2016). Hydrodynamic versus GIS modelling for coastal flood vulnerability assessment: Which is better for guiding coastal management?. *Ocean & Coastal Management*, 120, 99-109.
- Smiley, K. T. (2020). Social inequalities in flooding inside and outside of floodplains during Hurricane Harvey. *Environmental Research Letters*, 15(9), 0940b3.
- Smith, D. I. (1994). Flood damage estimation-A review of urban stage-damage curves and loss functions. *Water Sa*, 20(3), 231-238.
- Statista Search Department (2022, September 13th) Greater Houston metro area - GDP 2001-2021 [Infographic]. Statista.
- Sugrue, T. J. (2014). *The origins of the urban crisis: Race and inequality in postwar detroit*-updated edition (Vol. 168). Princeton University Press.
- Sun, A. Y., Xia, Y., Caldwell, T. G., & Hao, Z. (2018). Patterns of precipitation and soil moisture extremes in Texas, US: A complex network analysis. *Advances in water resources*, 112, 203-213.
- Tiné, M., Perez, L., Molowny-Horas, R., & Darveau, M. (2019). Hybrid spatiotemporal simulation of future changes in open wetlands: A study of the Abitibi-Témiscamingue region, Québec, Canada. *International journal of applied earth observation and geoinformation*, 74, 302-313.
- United Nations. 2014. *World Urbanization Prospects: The 2014 Revision, Highlights*. ST/ESA/SER.A/352, United Nations, Department of Economic and Social Affairs, Population Division.
- United States Census Bureau . (2021). Harris County POVERTY STATUS IN THE PAST 12 MONTHS. Retrieved August 22, 2023,.
- United States Census Bureau. (2021). Chambers County POVERTY STATUS IN THE PAST 12 MONTHS. Retrieved August 22, 2023,.
- United States Census Bureau. (2021). Galveston County POVERTY STATUS IN THE PAST 12 MONTHS. Retrieved August 22, 2023,.
- United States Geological Survey (2021). United States Geological Survey 3D Elevation Program 1/3 arc-second Digital Elevation Model. Distributed by OpenTopography. <https://doi.org/10.5069/G98K778D>. Accessed: 2023-06-06
- Vojinovic, Z., & Abbott, M. B. (2012). *Flood risk and social justice*. IWA Publishing.
- Wing, O.E.J., Lehman, W., Bates, P.D. et al. Inequitable patterns of US flood risk in the Anthropocene. *Nat. Clim. Chang.* 12, 156–162 (2022). <https://doi.org/10.1038/s41558-021-01265-6>

- Wu, W., Emerton, R., Duan, Q., Wood, A. W., Wetterhall, F., & Robertson, D. E. (2020). Ensemble flood forecasting: Current status and future opportunities. *Wiley Interdisciplinary Reviews: Water*, 7(3), e1432
- Xu, H., Ma, C., Xu, K., Lian, J., & Long, Y. (2020). Staged optimization of urban drainage systems considering climate change and hydrological model uncertainty. *Journal of Hydrology*, 587, 124959.
- You, H., & Potter, L. (2020). (rep.). Projections of the Total Population of Texas and Counties in Texas, 2020-2060 (pp. 2–9). San Antonio, Texas: The University of Texas .
- Zhang, S., & Pan, B. (2014). An urban storm-inundation simulation method based on GIS. *Journal of hydrology*, 517, 260-268.

## Appendix A: Data

Data Name	Year (s)	Spatial Resolution (m)	Filetype	Source	Additional Information
Topography	2021	10x10	Raster	USGS, 2021	
Subsidence Rates	2022	n/a	Point	USGS, Ramage, and Adams, 2022	
Storm Surge Predictions	2018	n/a	Integer	Bass et al., 2018	
RCP SLR Rates	2021	n/a	Integer	Miller & Shirzaei, 2021	
SLR Validation Extents	2022	n/a	Vector	NOAA, 2022	
Land Use	1985-2018	30x30	Raster	USGS - Pengra et al., 2022	Included Classes: Developed, Cropland, Grass/Shrub, Water, Tree Cover, Wetland, Ice/Snow, Barren
Demographic Composition and Distribution	2020	n/a	Vector	CDC/ATSDR, 2020	
Population Projections	2020-2060	n/a	Integer	Texas Demographic Center, 2020	
Flood Depth-Damage	2017	n/a	Integer	EU - Huizinga et al., 2017	

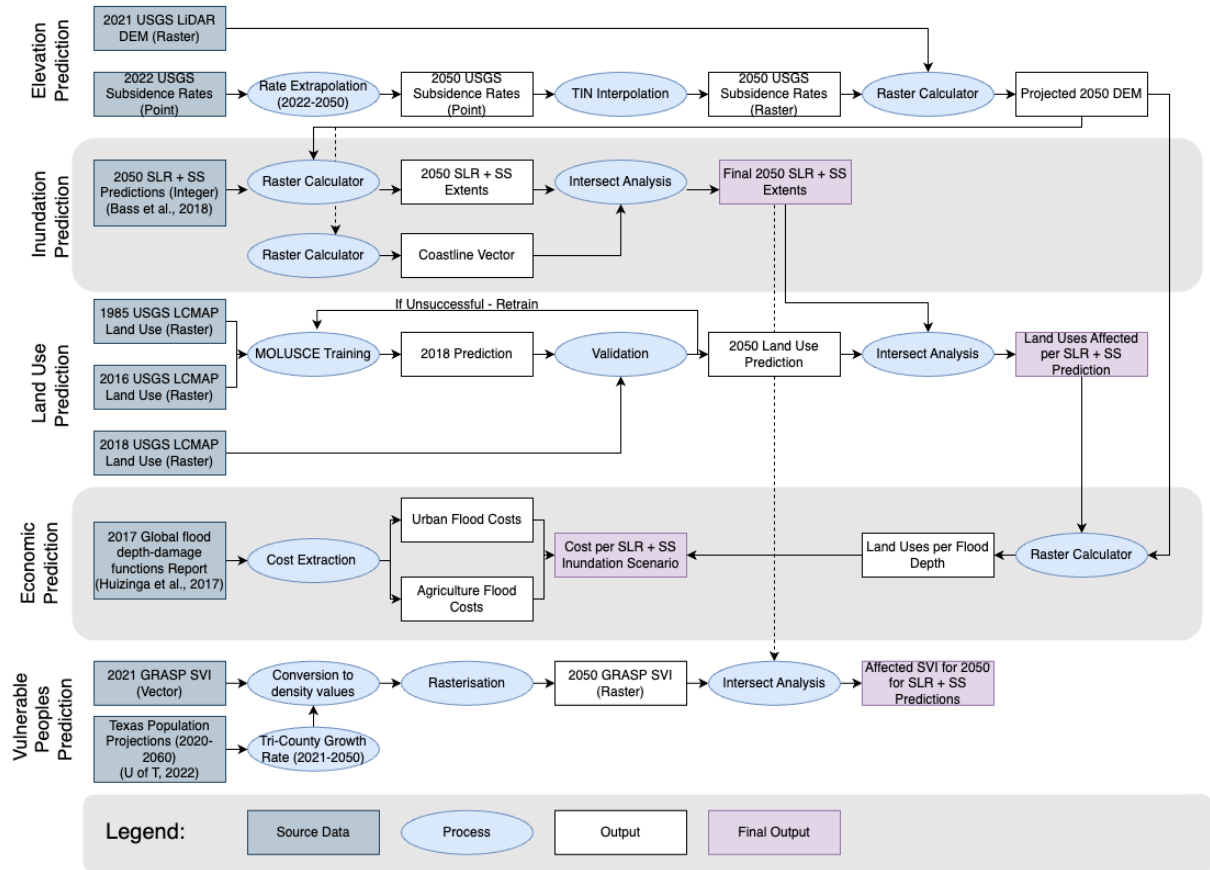


Figure 1: Geographic Information Systems Approach and Methods

## Appendix B: Flood Cost Enumeration

Table 1: Costs per inundated area, by depth, on the basis of Cost-Depth curves.

Land Use Type	Costs per inundation depth (eur/m <sup>2</sup> )							MOE (eur/m <sup>2</sup> )
	0.5	1.5	2.5	3.5	4.5	5.5	6+	
Inundation depth [m]								
Agriculture	0.011	0.0209	0.0266	0.0304	0.0342	0.0361	0.038	0.0019
Residential	150	220	275	350	375	450	475	25
Commercial	100	200	250	425	575	700	800	50
Industrial	190	250	400	500	570	580	600	50
Developed (Average)	146.67	223.33	308.33	425.00	506.67	576.67	625	41.66

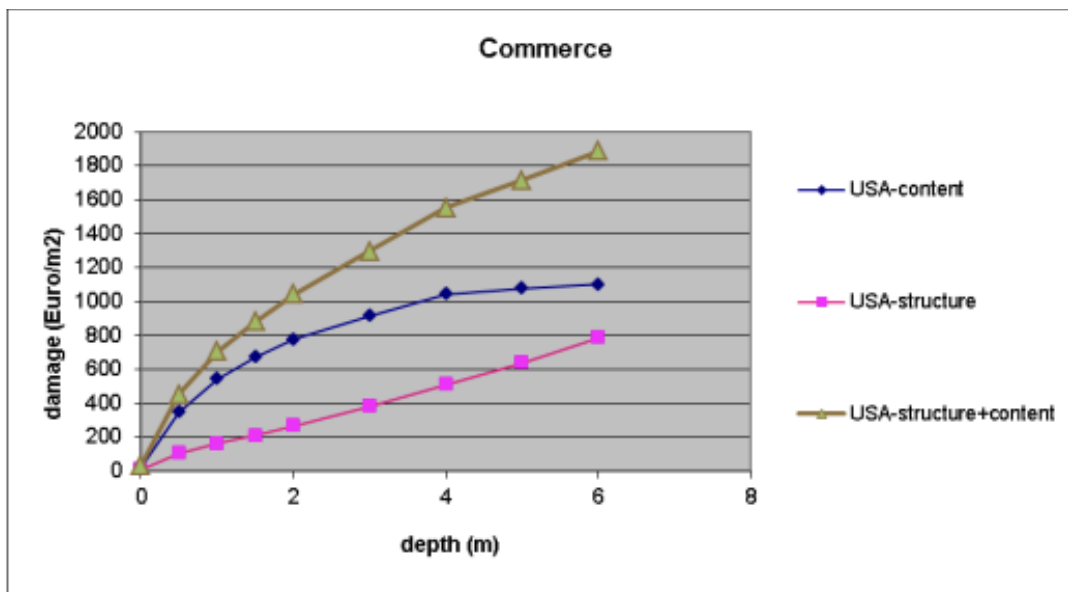


Figure 1: Cost (€) per m<sup>2</sup> for Commercial Buildings in North America - Structure and Content (Huizinga, De Moel, & Szewczyk, 2017)

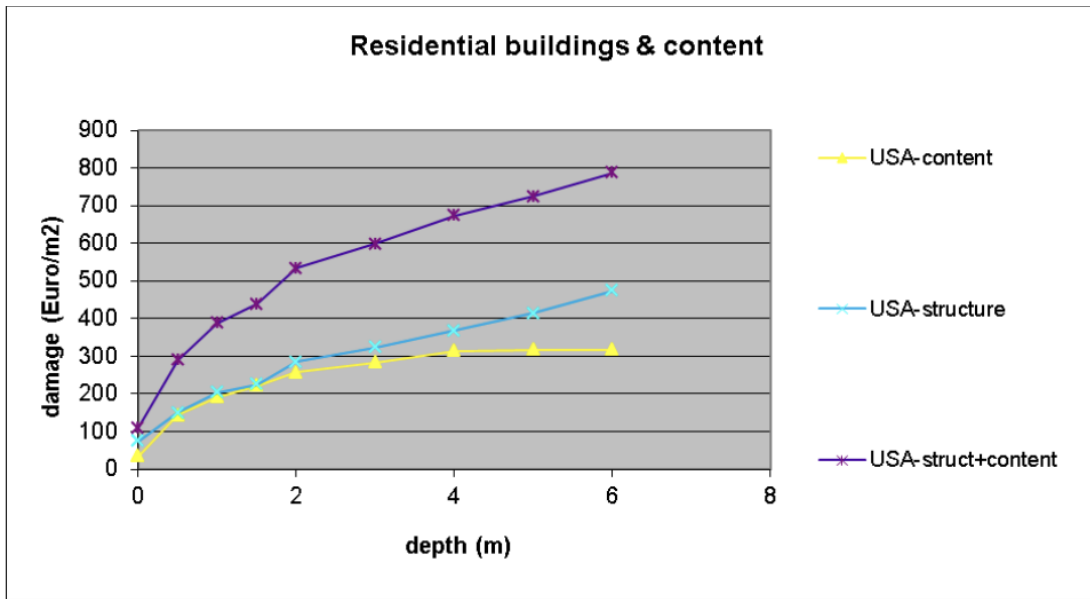


Figure 2: Cost (€) per m<sup>2</sup> for Residential Buildings in North America - Structure and Content (Huizinga, De Moel, & Szewczyk, 2017)

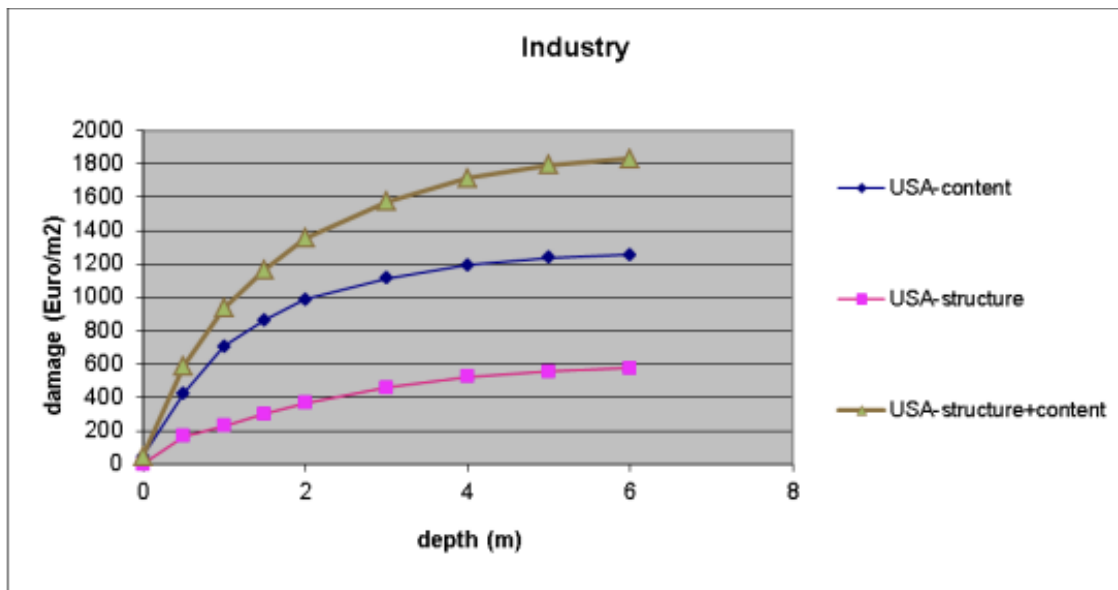


Figure 3: Cost (€) per m<sup>2</sup> for Industrial Buildings in North America - Structure and Content (Huizinga, De Moel, & Szewczyk, 2017)

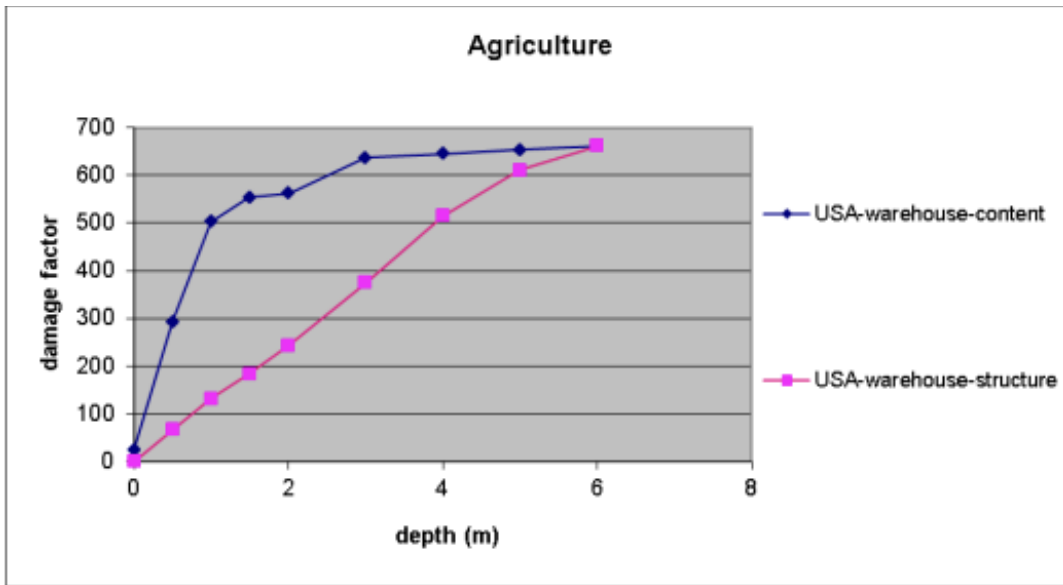


Figure 4: Damage Factor per  $m^2$  for Agriculture in North America  
(Huizinga, De Moel, & Szewczyk, 2017)



## Appendix C: Results

Table 1: Inundation Areas, by Land Use, Across RCP's

RCP and SLR Extent	RCP2.6 - 0.25m		RCP 4.0/6.0 - 0.26m		RCP 8.5 - 0.32m	
Land Use	Area (m <sup>2</sup> )	Proportion (%)	Area (m <sup>2</sup> )	Proportion	Area (m <sup>2</sup> )	Proportion (%)
Developed	74,000	5.749	75,000	5.799	85,000	5.857
Cropland	15,000	1.136	15,000	1.202	16,000	1.121
Grass/Shrub	116,000	9.084	118,000	9.194	160,000.000	10.966
Tree Cover	8,000	0.639	8,000	0.636	8,000	0.561
Wetland	43,000	3.336	43,000	3.324	55,000	3.738
Barren	1,026,000	80.057	1,027,000	79.844	1,135,000	77.757
Water	13,447,522,000		13,447,768,000		13,483,293,000	
			0		0	
Sum (sans water)	1,282,000		1,286,000		1,459,000	

Table 2: Inundation Areas, by Land Use, Across RCP's and Storm Surge Predictions

RCP and SLR Extent		RCP 2.6 - 0.25m							
Storm Surge	0.5 meters		2 meters		4 meters		8 meters		
Land Use	Area (m <sup>2</sup> )	Proportion (%)	Area (m <sup>2</sup> )	Proportion (%)	Area (m <sup>2</sup> )	Proportion (%)	Area (m <sup>2</sup> )	Proportion (%)	
Developed	113,000	6.388	9,892,000	17.622	114,981,000	11.587	489,291,000	23.876	
Cropland	19,000	1.082	898,000	1.600	134,993,000	13.604	579,191,000	28.263	
Grass/Shrub	198,000	11.231	613,000	1.092	22,955,000	2.313	47,877,000	2.336	
Tree Cover	9,000	0.515	160,000	0.285	4,500,000	0.454	46,157,000	2.252	
Wetland	83,000	4.688	18,332,000	32.657	644,218,000	64.922	796,916,000	38.888	
Barren	1,343,000	76.095	26,240,000	46.745	70,649,000	7.120	89,847,000	4.384	
Water	1,361,139,000		1,401,456,000		1,466,324,000		1,476,008,000		
Sum (sans water)	1,765,000		56,135,000		992,296,000		2,049,279,000		
RCP and SLR Extent		RCP 8.5 - 0.32m							
Storm Surge	0.5 meters		2 meters		4 meters		8 meters		
Land Use	Area (m <sup>2</sup> )	Proportion (%)	Area (m <sup>2</sup> )	Proportion (%)	Area (m <sup>2</sup> )	Proportion (%)	Area (m <sup>2</sup> )	Proportion (%)	
Developed	114,000	6.320	10,769,000	16.841	118,879,000	11.834	497,638,000	24.033	
Cropland	19,000	1.070	991,000	1.550	139,154,000	13.853	588,413,000	28.417	
Grass/Shrub	200,000	11.213	653,000	1.021	23,604,000	2.350	48,280,000	2.332	

Tree Cover	9,000	0.510	198,000	0.310	4,723,000	0.470	47,120,000	2.276
Wetland	87,000	4.893	23,698,000	37.058	647,201,000	64.428	799,109,000	38.592
Barren	1,356,000	75.994	27,640,000	43.221	70,976,000	7.066	90,095,000	4.351
Water	1,361,310,000		1,403,261,000		1,466,428,000		1,476,040,000	
-----								
Sum (sans water)	1,785,000		63,949,000		1,004,537,000		2,070,655,000	

Table 3: Inundated Land Uses (m<sup>2</sup>), per Surge Height

Land Use	Surge Height (m)									
	8+	7-8	6-7	5-6	4-5	3-4	2-3	1-2	0-1	
	Inundation Depth (m)									
	0-1	1-2	2-3	3-4	4-5	5-6	6-7	7-8	8+	
	RCP 2.6	RCP 8.6								
Developed	36,080,000	44,450,000	90,500,000	108,240,000	87,220,000	64,720,000	79,680,000	15,000,000	6,850,000	860,000
Cropland	56,900,000	66,080,000	87,990,000	131,820,000	115,540,000	69,110,000	114,010,000	3,280,000	540,000	80,000
Grass/Shrub	1,540,000	1,930,000	2,920,000	5,090,000	7,530,000	10,570,000	18,250,000	1,560,000	300,000	100,000
Tree Cover	3,670,000	4,650,000	9,000,000	13,990,000	10,620,000	4,560,000	2,910,000	1,100,000	140,000	40,000
Water	360,000	390,000	1,080,000	1,360,000	5,030,000	2,760,000	44,590,000	57,650,000	13,850,000	7,590,000
Wetland	10,430,000	12,630,000	22,750,000	39,960,000	47,060,000	43,240,000	512,070,000	112,050,000	6,430,000	2,400,000
Barren	1,180,000	1,420,000	3,620,000	4,810,000	5,580,000	4,950,000	27,480,000	25,960,000	12,810,000	2,440,000

Table 4: Economic Predictions (in euro) of Maximum and Minimum Storm Surge Scenarios, across Land Uses and RCP's

	Land Use	Inundation Depth (m)	0-1	1-2	2-3	3-4	4-5	5-6	6<
RCP 2.6 0.5m	Developed	Area (m <sup>2</sup> )	113,000	-	-	-	-	-	-
		Depth Cost (€/m <sup>2</sup> )	146.67	-	-	-	-	-	-
		Cost (€)	16,573,710	-	-	-	-	-	-
	Agriculture	Area (m <sup>2</sup> )	19,000	-	-	-	-	-	-
		Depth Cost (€/m <sup>2</sup> )	56.90	-	-	-	-	-	-
		Cost (€)	1,081,100	-	-	-	-	-	-
<b>Total (€)</b>			17,654,810						
RCP 8.5 0.5m	Developed	Area (km <sup>2</sup> )	0.114	-	-	-	-	-	-
		Depth Cost (€/m <sup>2</sup> )	146.67	-	-	-	-	-	-
		Cost (€)	16,720,380	-	-	-	-	-	-
	Agriculture	Area (m <sup>2</sup> )	19,000	-	-	-	-	-	-
		Depth Cost (€/m <sup>2</sup> )	56.90	-	-	-	-	-	-
		Cost (€)	1,081,100	-	-	-	-	-	-
<b>Total (€)</b>			17,801,480						
RCP 2.6 8m	Developed	Area (m <sup>2</sup> )	36,080,000	90,500,000	108,240,000	87,220,000	64,720,000	79,680,000	22,710,000
		Depth Cost (€/m <sup>2</sup> )	146.67	223.33	308.33	425.00	506.67	576.67	625
		Cost (€)	5,291,853,600	20,211,365,000	33,373,639,200	37,068,500,000	32,791,682,400	45,949,065,600	14,193,750,000
	Agriculture	Area (m <sup>2</sup> )	56,900,000	87,990,000	131,820,000	115,540,000	69,110,000	114,010,000	3,900,000
		Depth Cost (€/m <sup>2</sup> )	0.011	0.0209	0.0266	0.0304	0.0342	0.0361	0.038
		Cost (€)	625,900	1,838,991	3,506,412	3,512,416	2,363,562	4,115,761	148,200
<b>Total (€)</b>			188,895,967,042						
RCP 8.5 8m	Developed	Area (m <sup>2</sup> )	44,450,000	90,500,000	108,240,000	87,220,000	64,720,000	79,680,000	22,710,000
		Depth Cost (€/m <sup>2</sup> )	146.67	223.33	308.33	425.00	506.67	576.67	625
		Cost (€)	6,519,481,500	20,211,365,000	33,373,639,200	37,068,500,000	32,791,682,400	45,949,065,600	14,193,750,000

		00	000	200	000	400	600	000
Agriculture	Area (m <sup>2</sup> )	66,080,000	87,990,000	131,820,000	115,540,000	69,110,000	114,010,000	3,900,000
	Depth Cost (€/m <sup>2</sup> )	56.90	66.08	87.99	131.82	115.54	69.11	114.01
	Cost (€)	3,759,952,000	5,814,379,200	11,598,841,800	15,230,482,800	7,984,969,400	7,879,231,100	444,639,000
<b>Total (€)</b>		242,819,979,000						

Table 5: MOLUSCE-Generated Predicted Land Use Transition for 2050

Land Use	Land Use Year		Change (m <sup>2</sup> )
	2022	2050	
Developed	3,472,680,995.44	3,504,421,217.33	31,740,221.89
Cropland	1,728,924,469.83	1,752,584,937.65	23,660,467.82
Grass/Shrub	140,984,069.15	108,828,625.20	-32,155,443.95
Tree	332,587,482.99	311,974,673.24	-20,612,809.75
Water	1,539,870,807.09	1,537,601,465.71	-2,269,341.38
Wetland	1,194,921,030.75	1,193,950,381.76	-970,648.99
Barren	172,693,733.57	173,301,287.93	607,554.36

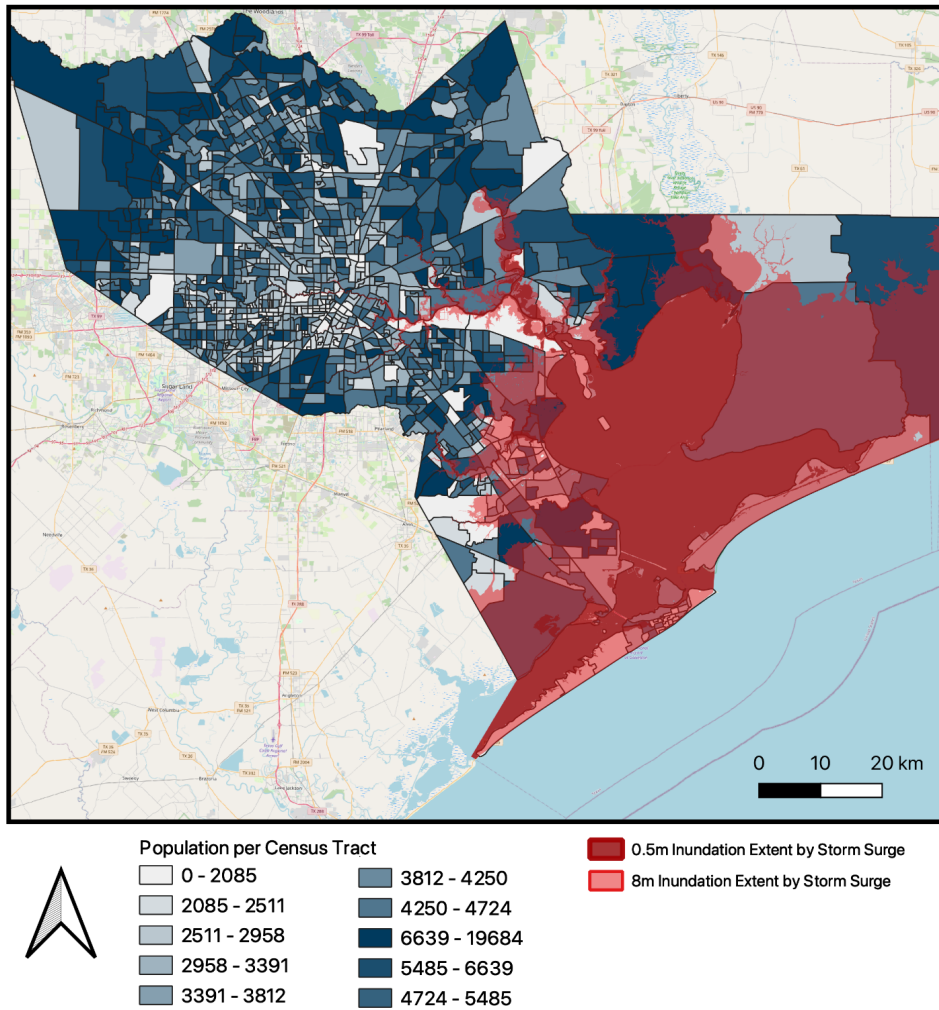


*Figure 1: Map of Projected Inundation of the Greater Houston Area in 2050, with Projected Subsidence, RCP8.5 Sea Level Rise, and 0.5m & 8m Storm Surge Prediction Applied. Base Density Map of Denizen Population*



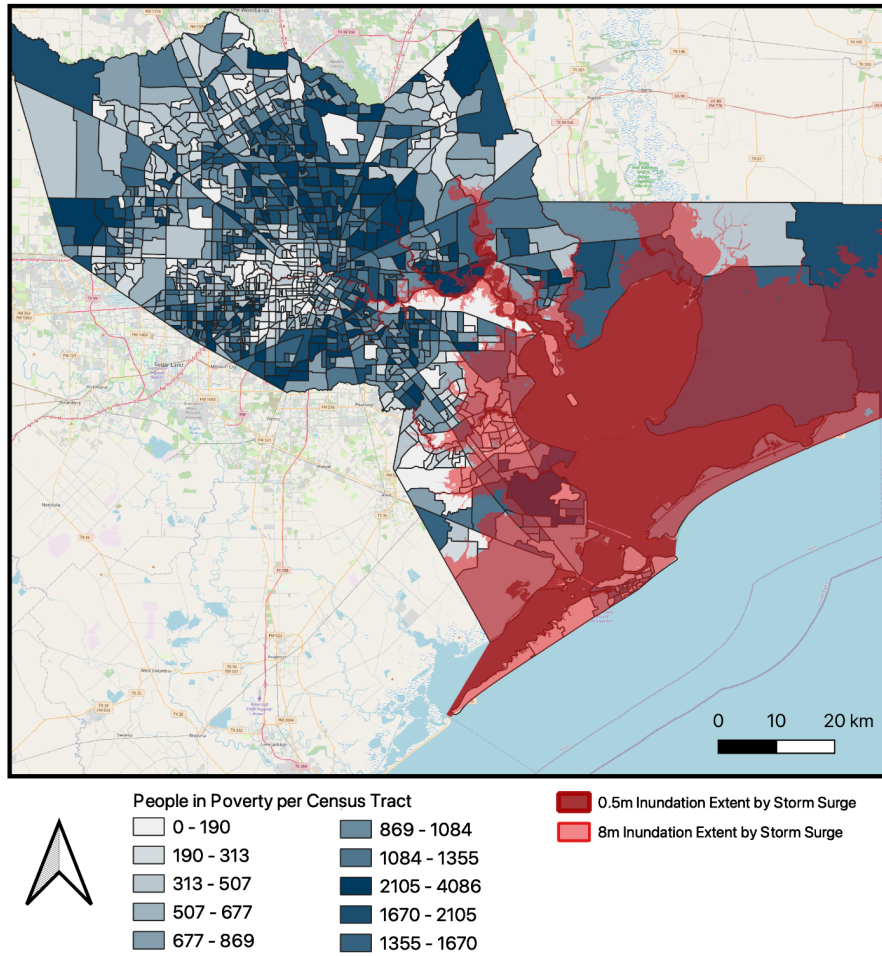


*Figure 2: Map of Projected Inundation of the Greater Houston Area in 2050, with Projected Subsidence, RCP8.5 Sea Level Rise, and 0.5m & 8m Storm Surge Prediction Applied. Base Density Map of Denizens in Poverty*

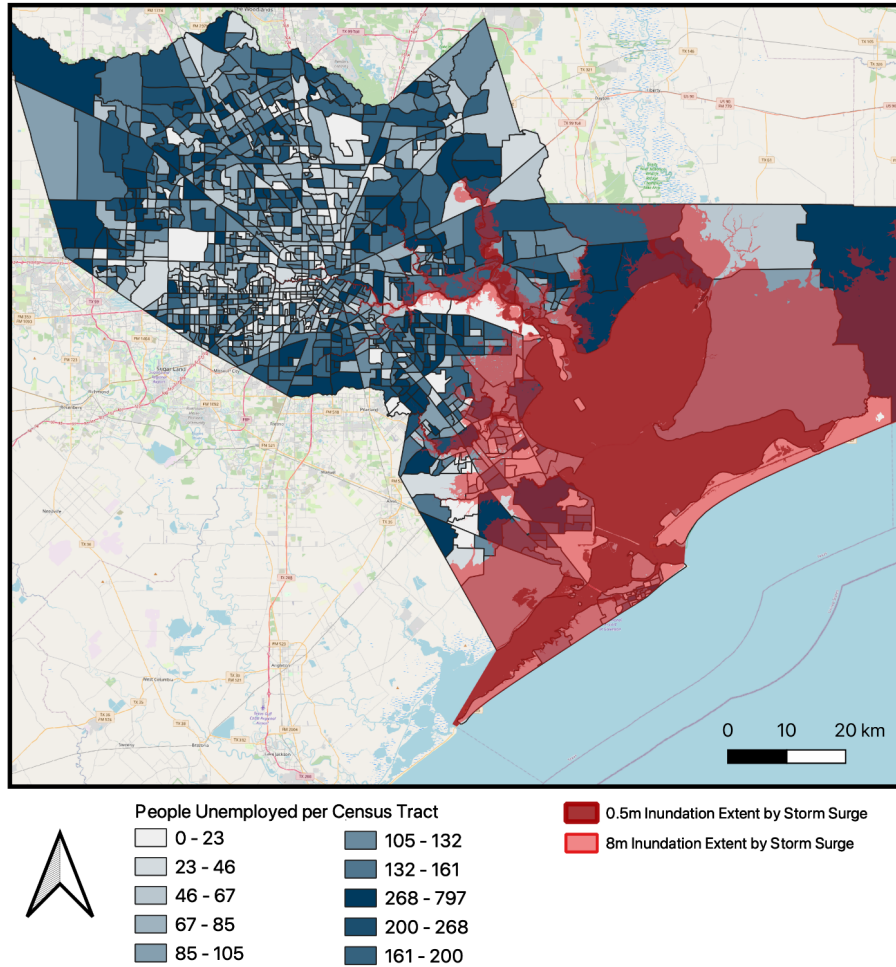


*Figure 3: Map of Projected Inundation of the Greater Houston Area in 2050, with Projected Subsidence, RCP8.5 Sea Level Rise, and 0.5m & 8m Storm Surge Prediction Applied. Base Density Map of Denizens Unemployed*

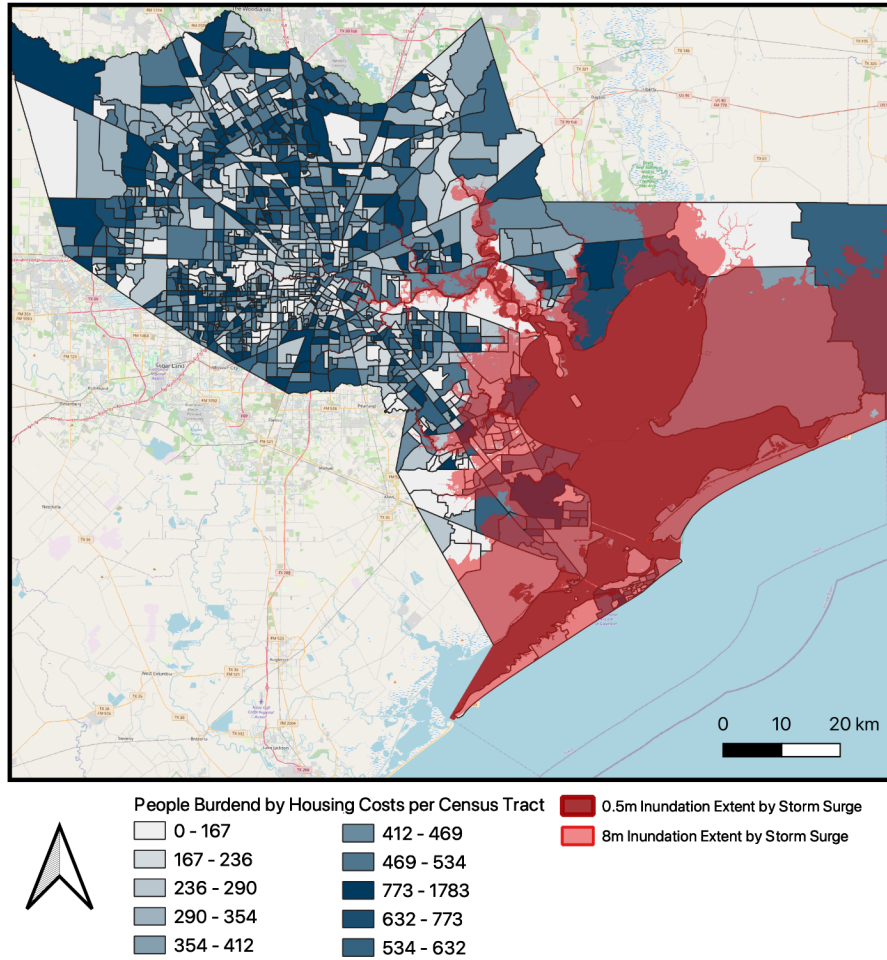


*Figure 4: Map of Projected Inundation of the Greater Houston Area in 2050, with Projected Subsidence, RCP8.5 Sea Level Rise, and 0.5m & 8m Storm Surge Prediction Applied. Base Density Map of Denizens Burdened by Housing Costs*

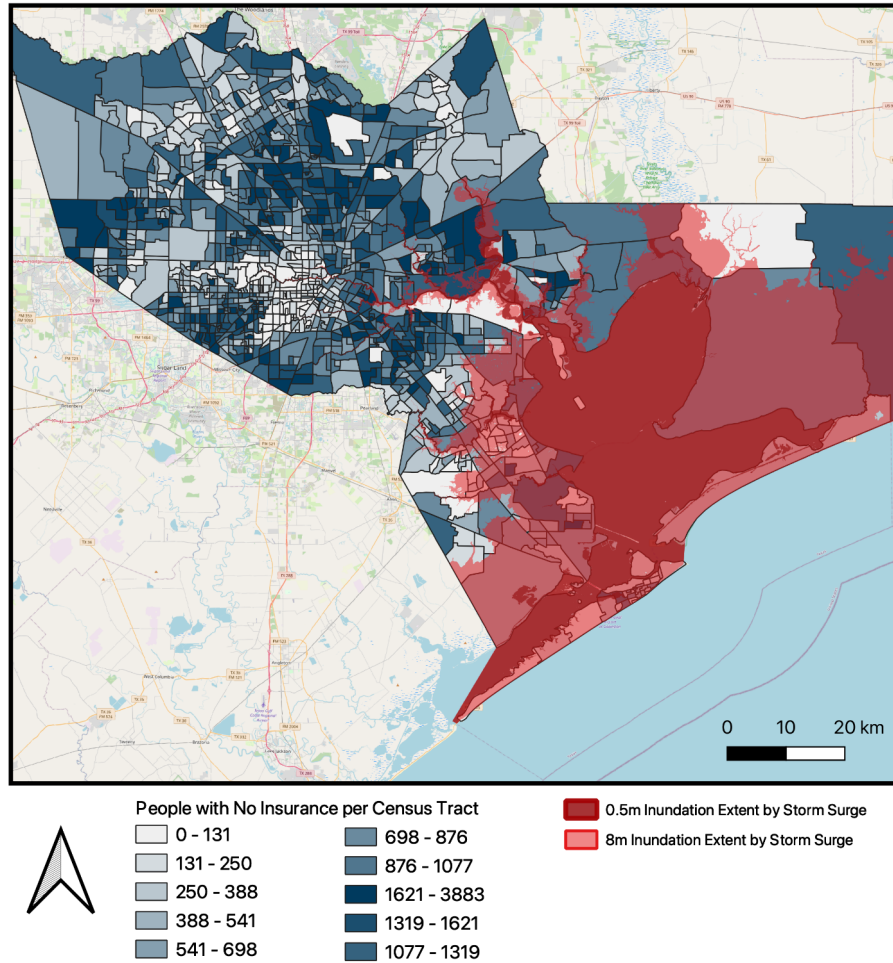


*Figure 5: Map of Projected Inundation of the Greater Houston Area in 2050, with Projected Subsidence, RCP8.5 Sea Level Rise, and 0.5m & 8m Storm Surge Prediction Applied. Base Density Map of Denizens with No Insurance*

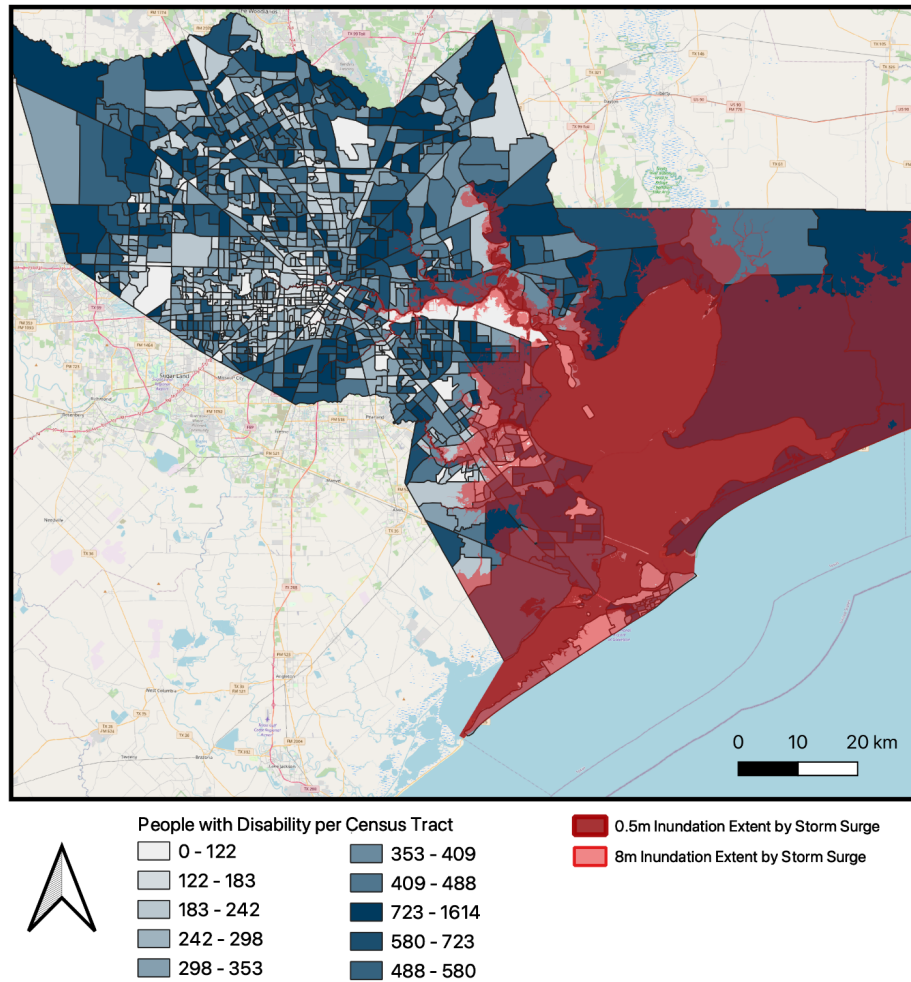


*Figure 6: Map of Projected Inundation of the Greater Houston Area in 2050, with Projected Subsidence, RCP8.5 Sea Level Rise, and 0.5m & 8m Storm Surge Prediction Applied. Base Density Map of Denizens with Disability*

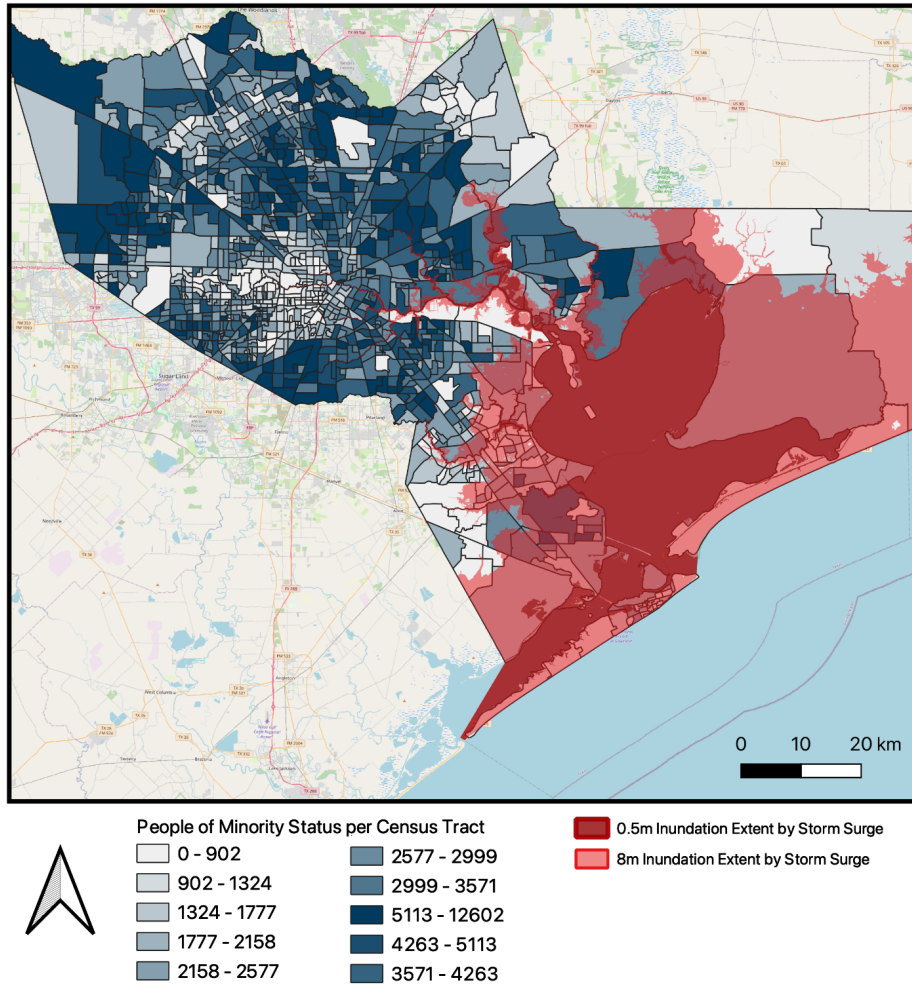


*Figure 7: Map of Projected Inundation of the Greater Houston Area in 2050, with Projected Subsidence, RCP8.5 Sea Level Rise, and 0.5m & 8m Storm Surge Prediction Applied. Base Density Map of Denizens with Minority Status*

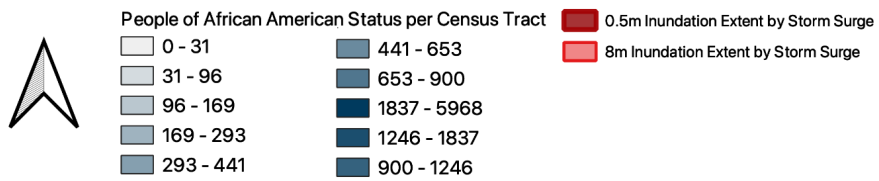
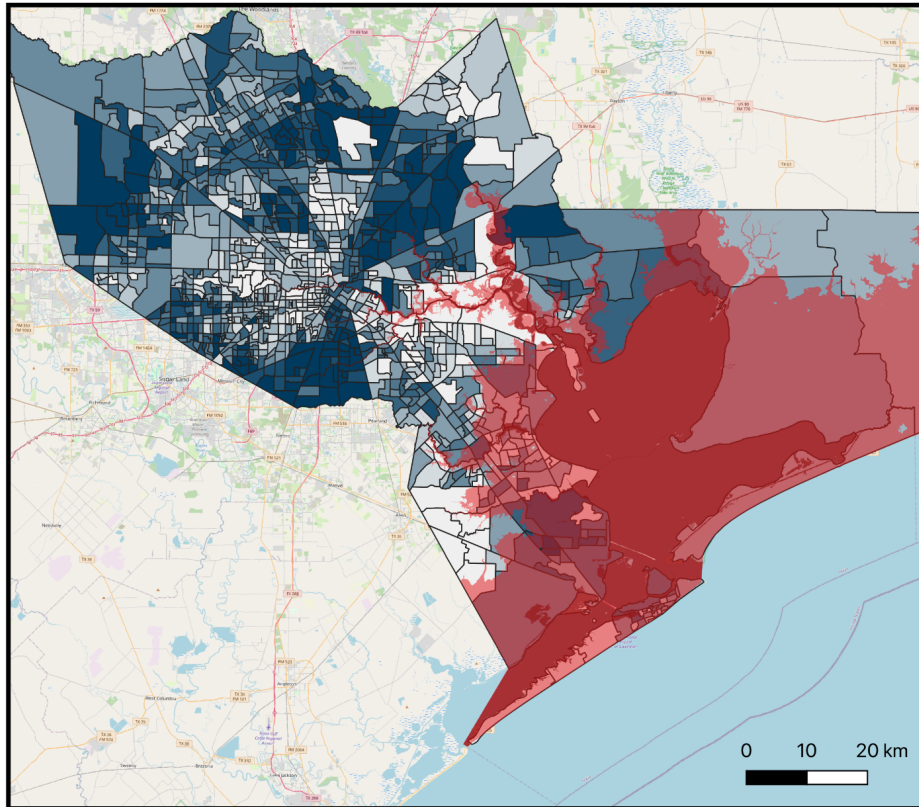


*Figure 8: Map of Projected Inundation of the Greater Houston Area in 2050, with Projected Subsidence, RCP8.5 Sea Level Rise, and 0.5m & 8m Storm Surge Prediction Applied. Base Density Map of Denizens with African American Status*

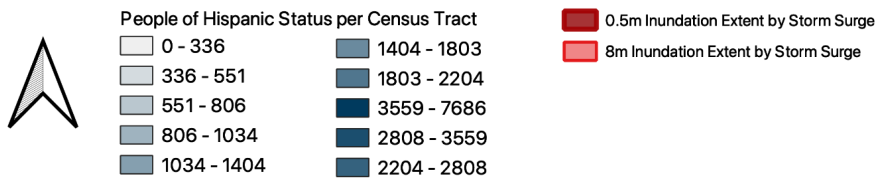
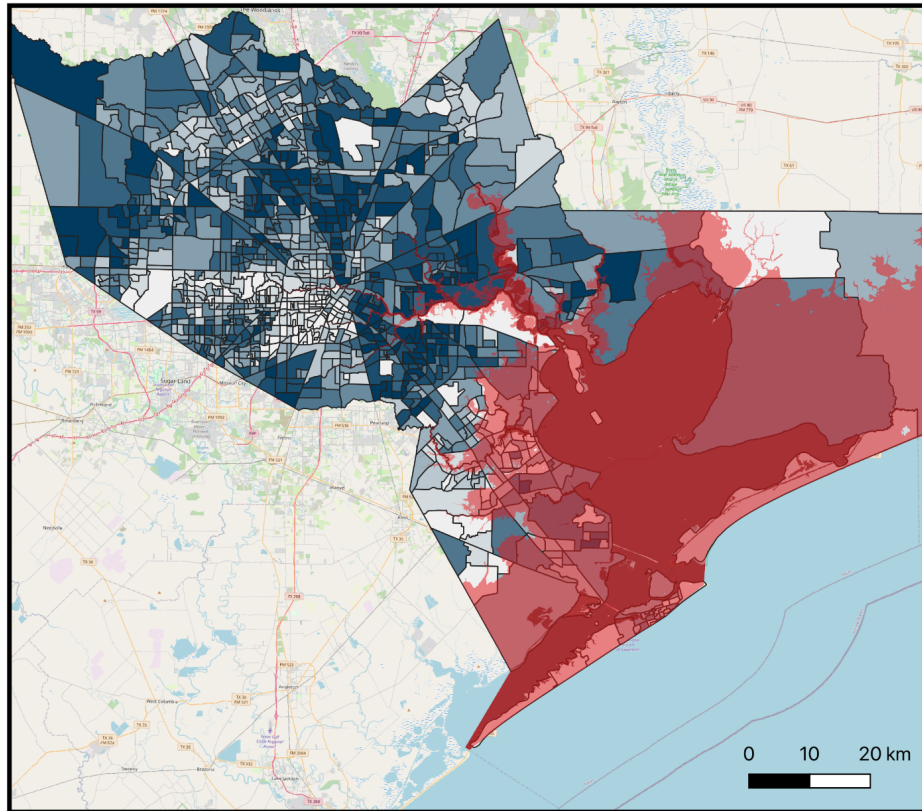


*Figure 9: Map of Projected Inundation of the Greater Houston Area in 2050, with Projected Subsidence, RCP8.5 Sea Level Rise, and 0.5m & 8m Storm Surge Prediction Applied. Base Density Map of Denizens with Hispanic Status*



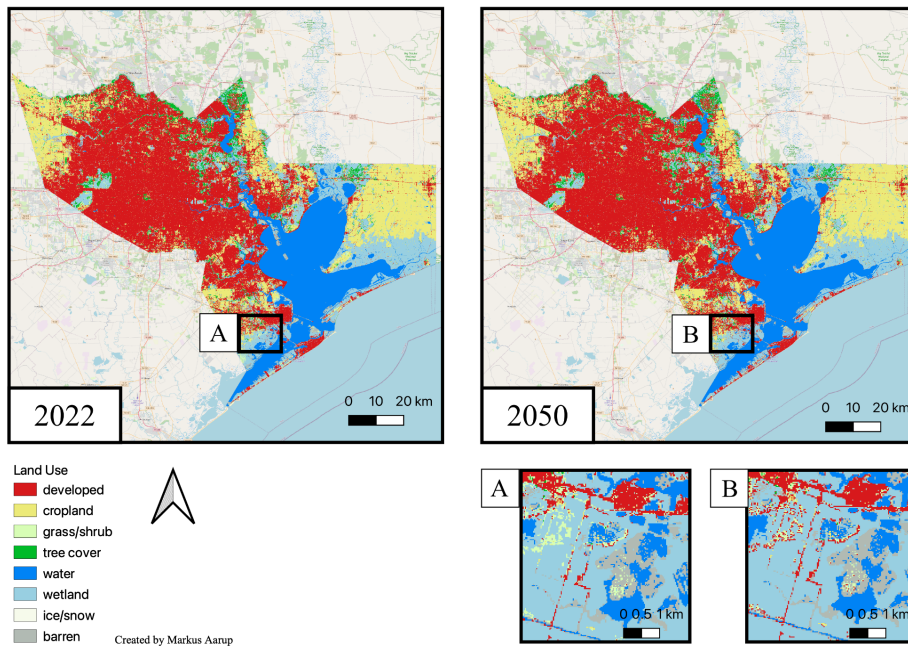


*Figure 10: MOLUSCE Predicted Output for 2050 Land Use Transition*

### ***Appendix D: IHS copyright form***

In order to allow the IHS Research Committee to select and publish the best UMD theses, students need to sign and hand in this copyright form to the course bureau together with their final thesis.

By signing this form, you agree that you are the sole author(s) of the work and that you have the right to transfer copyright to IHS, except for those items clearly cited or quoted in your work.

Criteria for publishing:

1. A summary of 400 words must be included in the thesis.
2. The number of pages for the thesis does not exceed the maximum word count.
3. The thesis is edited for English.

Please consider the length restrictions for the thesis. The Research Committee may elect not to publish very long and/or poorly written theses.

I grant IHS, or its successors, all copyright to the work listed above, so that IHS may publish the work in the IHS Thesis Series, on the IHS web site, in an electronic publication or in any other medium.

IHS is granted the right to approve reprinting.


The author retains the rights to create derivative works and to distribute the work cited above within the institution that employs the author.

Please note that IHS copyrighted material from the IHS Thesis Series may be reproduced, up to ten copies for educational (excluding course packs purchased by students), non-commercial purposes, provided a full acknowledgement and a copyright notice appear on all reproductions.

Thank you for your contribution to IHS.

Date : 21.08.2023

Your Name(s) : Markus Aarup

Your Signature(s) : 

Please direct this form and all questions regarding this form or IHS copyright policy to:

Academic Director Burg. Oudlaan 50, T-Building 14 <sup>th</sup> floor, 3062 PA Rotterdam, The Netherlands	<a href="mailto:gerrits@Ihs.nl">gerrits@Ihs.nl</a> Tel. +31 10 4089825
--	---

**IHS**  
Making cities work

Houston under Rising Seas: Social and Economic Implications of Climate Change for 2050



Institute for Housing and  
Urban Development Studies of  
Erasmus University Rotterdam